

1 SEARCH FOR PRODUCTION OF A HIGGS BOSON AND A SINGLE TOP  
2 QUARK IN MULTILEPTON FINAL STATES IN  $pp$  COLLISIONS AT  $\sqrt{s} = 13$   
3 TeV.

4 by

5 Jose Andres Monroy Montañez

6 A DISSERTATION

7 Presented to the Faculty of

8 The Graduate College at the University of Nebraska

9 In Partial Fulfilment of Requirements

10 For the Degree of Doctor of Philosophy

11 Major: Physics and Astronomy

12 Under the Supervision of Kenneth Bloom and Aaron Dominguez

13 Lincoln, Nebraska

14 July, 2018

15 SEARCH FOR PRODUCTION OF A HIGGS BOSON AND A SINGLE TOP  
16 QUARK IN MULTILEPTON FINAL STATES IN  $pp$  COLLISIONS AT  $\sqrt{s} = 13$   
17 TeV.

18 Jose Andres Monroy Montañez, Ph.D.

19 University of Nebraska, 2018

20 Adviser: Kenneth Bloom and Aaron Dominguez

# Table of Contents

22	<b>Table of Contents</b>	<b>iii</b>
23	<b>List of Figures</b>	<b>vi</b>
24	<b>List of Tables</b>	<b>viii</b>
25	<b>1 INTRODUCTION</b>	<b>1</b>
26	<b>2 Theoretical approach</b>	<b>2</b>
27	2.1 Introduction . . . . .	2
28	2.2 Standard model of particle physics . . . . .	3
29	2.2.1 Fermions . . . . .	5
30	2.2.1.1 Leptons . . . . .	6
31	2.2.1.2 Quarks . . . . .	8
32	2.2.2 Fundamental interactions . . . . .	12
33	2.2.3 Gauge bosons . . . . .	18
34	2.3 Electroweak unification and the Higgs mechanism . . . . .	20
35	2.3.1 Spontaneous symmetry breaking (SSB) . . . . .	28
36	2.3.2 Higgs mechanism . . . . .	32
37	2.3.3 Masses of the gauge bosons . . . . .	34

38	2.3.4	Masses of the fermions . . . . .	35
39	2.3.5	The Higgs field . . . . .	36
40	2.3.6	Production of Higgs bosons at LHC . . . . .	37
41	2.3.7	Higgs boson decay channels . . . . .	41
42	2.4	Associated production of a Higgs boson and a single Top quark. . . .	42
43	2.5	The CP-mixing in tH processes . . . . .	47
44	2.6	Experimantal status of the anomalous Higg-fermion coupling. . . . .	51
45		<b>Bibliography</b>	<b>52</b>
46		<b>References</b>	<b>53</b>

## 47 List of Figures

48	2.1	Standard model of particle physics. . . . .	4
49	2.2	Transformations between quarks . . . . .	12
50	2.3	Fundamental interactions in nature. . . . .	13
51	2.4	SM interactions diagrams . . . . .	14
52	2.5	Neutral current processes . . . . .	21
53	2.6	Spontaneous symmetry breaking mechanism . . . . .	28
54	2.7	SSB Potential form . . . . .	29
55	2.8	Potential for complex scalar field . . . . .	30
56	2.9	SSB mechanism for complex scalar field . . . . .	31
57	2.10	Proton-Proton collision . . . . .	38
58	2.11	Higgs boson production mechanism Feynman diagrams . . . . .	39
59	2.12	Higgs boson production cross section and decay branching ratios . . . . .	40
60	2.13	Associated Higgs boson production mechanism Feynman diagrams . . . . .	43
61	2.14	Cross section for tHq process as a function of $\kappa_t$ . . . . .	45
62	2.15	Cross section for $tHW$ process as a function of $\kappa_{Htt}$ . . . . .	46
63	2.16	NLO cross section for $tX_0$ and $t\bar{t}X_0$ . . . . .	49
64	2.17	NLO cross section for $tWX_0$ , $t\bar{t}X_0$ . . . . .	50

65	2.18 Two dimensional $\kappa_t$ - $\kappa_V$ plot of the coupling modifiers. ATLAS and CMS	
66	combination. . . . .	51

## 67 List of Tables

68	2.1	Fermions of the SM. . . . .	5
69	2.2	Fermion masses. . . . .	6
70	2.3	Leptons properties. . . . .	9
71	2.4	Quarks properties. . . . .	9
72	2.5	Fermion weak isospin and weak hypercharge multiplets. . . . .	11
73	2.6	Fundamental interactions features. . . . .	15
74	2.7	SM gauge bosons. . . . .	19
75	2.8	Higgs boson properties. . . . .	37
76	2.9	Predicted branching ratios for a SM Higgs boson with $m_H = 125 \text{ GeV}/c^2$ . . . . .	42
77	2.10	Predicted SM cross sections for tH production at $\sqrt{s} = 13 \text{ TeV}$ . . . . .	44
78	2.11	Predicted enhancement of the $tHq$ and $tHW$ cross sections at LHC . . . . .	47

## <sup>79</sup> Chapter 1

## <sup>80</sup> INTRODUCTION



## Chapter 2

### Theoretical approach

#### 2.1 Introduction

The physical description of the universe is a challenge that physicists have faced by making theories that refine existing principles and proposing new ones in an attempt to embrace emerging facts and phenomena.

At the end of 1940s Julian Schwinger [1] and Richard P. Feynman [2], based in the work of Sin-Itiro Tomonaga [3], developed an electromagnetic theory consistent with special relativity and quantum mechanics that describes how matter and light interact; the so-called “quantum eletrodynamics” (QED) had born.

QED has become the guide in the development of theories that describe the universe. It was the first example of a quantum field theory (QFT), which is the theoretical framework for building quantum mechanical models that describes particles and their interactions. QFT is composed of a set of mathematical tools that combines classical fields, special relativity and quantum mechanics, while keeping the quantum point

98 particles and locality ideas.

99 This chapter gives an overview of the standard model of particle physics, starting  
 100 with a description of the particles and interactions that compose it, followed by a  
 101 description of the electroweak interaction, the Higgs boson and the associated pro-  
 102 duction of Higgs boson and a single top quark ( $tH$ ). The description contained in  
 103 this chapter is based on references [4–6].

## 104 **2.2 Standard model of particle physics**

105 Particle physics at the fundamental level is modeled in terms of a collection of in-  
 106 teracting particles and fields in a theory known as the “standard model of particle  
 107 physics (SM)”<sup>1</sup>.

108

109 The full picture of the SM is composed of three fields<sup>2</sup>, whose excitations are inter-  
 110 preted as particles called mediators or force-carriers; a set of fields, whose excitations  
 111 are interpreted as elementary particles, interacting through the exchange of those  
 112 mediators and a field that gives the mass to elementary particles. Figure 2.1 shows  
 113 an scheme of the SM particles organization. In addition to the particles in the scheme  
 114 (but not listed in it), their corresponding anti-particles, with opposite quantum num-  
 115 bers, are also part of the picture; some particles are their own anti-particles, like  
 116 photon or Higgs, or anti-particle is already listed like in the  $W^+$  and  $W^-$  case.

117

118 The mathematical formulation of the SM is based on group theory and the use of  
 119 Noether’s theorem [8] which states that for a physical system modeled by a Lagrangian

---

<sup>1</sup> The formal and complete treatment of the SM is out of the scope of this document, however a plenty of textbooks describing it at several levels are available in the literature. The treatment in references [?] is quite comprehensive and detailed.

<sup>2</sup> Note that gravitational field is not included in the standard model formulation

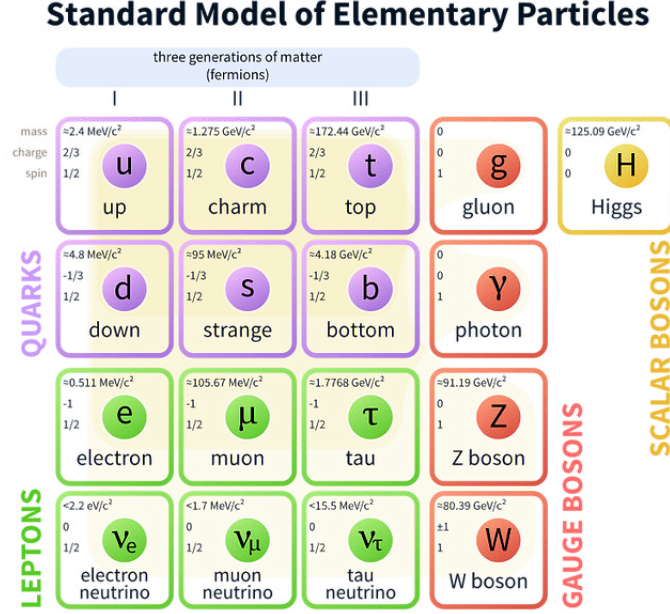


**Figure 2.1:** Schematic representation of the Standard model of particle physics. SM is a theoretical model intended to describe three of the four fundamental forces of the universe in terms of a set of particles and their interactions. [7].

that is invariant under a group of transformations a conservation law is expected. For instance, a system described by a time-independent Lagrangian is invariant (symmetric) under time changes (transformations) with the total energy conservation law as the expected conservation law. In QED, the charge operator ( $Q$ ) is the generator of the  $U(1)$  symmetry which according to the Noether's theorem means that there is a conserved quantity; this conserved quantity is the electric charge and thus the law conservation of electric charge is established.

127

In the SM, the symmetry group  $SU(3)_C \otimes SU(2)_L \otimes U(1)_Y$  describes three of the four fundamental interactions in nature (see section 2.2.2): strong interaction (SI), weak interaction (WI) and electromagnetic interactions (EI) in terms of symmetries associated to physical quantities:

131

- 132 • Strong:  $SU(3)_C$  associated to color charge
- 133 • Weak:  $SU(2)_L$  associated to weak isospin and chirality
- 134 • Electromagnetic:  $U(1)_Y$  associated to weak hypercharge and electric charge

135 It will be shown that the electromagnetic and weak interactions are combined in  
 136 the so-called electroweak interaction where chirality, hypercharge, weak isospin and  
 137 electric charge are the central concepts.

### 138 2.2.1 Fermions

139 The basic constituents of the ordinary matter at the lowest level, which form the set  
 140 of elementary particles in the SM formulation, are quarks and leptons. All of them  
 141 have spin 1/2, therefore they are classified as fermions since they obey Fermi-Dirac  
 142 statistics. There are six “flavors” of quarks and three of leptons organized in three  
 143 generations, or families, as shown in table 2.1.

144

		Generation		
	Type	1st	2nd	3rd
Leptons	Charged	Electron (e)	Moun( $\mu$ )	Tau ( $\tau$ )
	Neutral	Electron neutrino ( $\nu_e$ )	Muon neutrino ( $\nu_\mu$ )	Tau neutrino ( $\nu_\tau$ )
Quarks	Up-type	Up (u)	Charm (c)	Top (t)
	Down-type	Down (d)	Strange (s)	Bottom (b)

**Table 2.1:** Fermions of the SM. There are six flavors of quarks and three of leptons, organized in three generations, or families, composed of two pairs of closely related particles. The close relationship is motivated by the fact that WI between leptons is limited to the members of the same generation; WI between quarks is not limited but greatly favoured, to same generation members.

145

146 There is a mass hierarchy between generations (see table 2.2), where the higher gener-  
 147 ation particles decays to the lower one, which can explain why the ordinary matter is

made of particles in the first generation. In the SM, neutrinos are modeled as massless particles so they are not subject to this mass hierarchy; however, today it is known that neutrinos are massive so the hierarchy could be restated. The reason behind this mass hierarchy is one of the most important open questions in particle physics, and it becomes more puzzling when noticing that the mass difference between first and second generation fermions is small compared to the mass difference with respect to the third generation.

Lepton	Mass (MeV/c <sup>2</sup> )	Quark	Mass (MeV/c <sup>2</sup> )
e	0.51	u	2.2
$\mu$	105.65	c	$1.28 \times 10^3$
$\tau$	1776.86	t	$173.1 \times 10^3$
$\nu_e$	Unknown	d	4.7
$\nu_\mu$	Unknown	s	96
$\tau_\mu$	Unknown	b	$4.18 \times 10^3$

**Table 2.2:** Fermion masses [9]. Generations differ by mass in a way that have been interpreted as a mass hierarchy. Approximate values with no uncertainties are used, for comparison purpose.

155

Usually, the second and third generation fermions are produced in high energy processes, like the ones recreated in particle accelerators.

### 2.2.1.1 Leptons

A lepton is an elementary particle that is not subject to the SI. As seen in table 2.1, there are two types of leptons, the charged ones (electron, muon and tau) and the neutral ones (the three neutrinos). The electric charge (Q) is the property that gives leptons the ability to participate in the EI. From the classical point of view, Q plays a central role determining, among others, the strength of the electric field through which the electromagnetic force is exerted. It is clear that neutrinos are not affected

165 by EI because they don't carry electric charge.

166

167 Another feature of the leptons that is fundamental in the mathematical description  
 168 of the SM is the chirality, which is closely related to spin and helicity. Helicity defines  
 169 the handedness of a particle by relating its spin and momentum such that if they  
 170 are parallel then the particle is right-handed; if spin and momentum are antiparallel  
 171 the particle is said to be left-handed. The study of parity conservation (or viola-  
 172 tion) in  $\beta$ -decay has shown that only left-handed electrons/neutrinos or right-handed  
 173 positrons/anti-neutrinos are created [10]; the inclusion of that feature in the theory  
 174 was achieved by using projection operators for helicity, however, helicity is frame de-  
 175 pendent for massive particles which makes it not Lorentz invariant and then another  
 176 related attribute has to be used: *chirality*.

177

178 Chirality is a purely quantum attribute which makes it not so easy to describe in  
 179 graphical terms but it defines how the wave function of a particle transforms under  
 180 certain rotations. As with helicity, there are two chiral states, left-handed chiral (L)  
 181 and right-handed chiral (R). In the highly relativistic limit where  $E \approx p \gg m$  helicity  
 182 and chirality converge, becoming exactly the same for massless particles.

183

184 In the following, when referring to left-handed (right-handed) it will mean left-handed  
 185 chiral (right-handed chiral). The fundamental fact about chirality is that while EI  
 186 and SI are not sensitive to chirality, in WI left-handed and right-handed fermions are  
 187 treated asymmetrically, such that only left handed fermions and right-handed anti-  
 188 fermions are allowed to couple to WI mediators, which is a violation of parity. The  
 189 way to translate this statement in a formal mathematical formulation is based on the  
 190 isospin symmetry group  $SU(2)_L$ .

191

192 Each generation of leptons is seen as a weak isospin doublet.<sup>3</sup> The left-handed charged  
 193 lepton and its associated left-handed neutrino are arranged in doublets of weak isospin  
 194  $T=1/2$  while their right-handed partners are singlets:

$$\begin{pmatrix} \nu_l \\ l \end{pmatrix}_L, l_R := \begin{pmatrix} \nu_e \\ e \end{pmatrix}_L, \begin{pmatrix} \nu_\mu \\ \mu \end{pmatrix}_L, \begin{pmatrix} \nu_\tau \\ \tau \end{pmatrix}_L, e_R, \mu_R, \tau_R, \nu_{eR}, \nu_{\mu R}, \nu_{\tau R} \quad (2.1)$$

195 The isospin third component refers to the eigenvalues of the weak isospin operator  
 196 which for doublets is  $T_3 = \pm 1/2$ , while for singlets it is  $T_3 = 0$ . The physical meaning  
 197 of this doublet-singlet arrangement falls in that the WI couples the two particles in  
 198 the doublet by exchanging the interaction mediator while the singlet member is not  
 199 involved in WI. The main properties of the leptons are summarized in table 2.3.

200

201 Although all three flavor neutrinos have been observed, their masses remain unknown  
 202 and only some estimations have been made [11]. The main reason is that the fla-  
 203 vor eigenstates are not the same as the mass eigenstates which implies that when  
 204 a neutrino is created its mass state is a linear combination of the three mass eigen-  
 205 states and experiments can only probe the squared difference of the masses. The  
 206 Pontecorvo-Maki-Nakagawa-Sakata (PMNS) mixing matrix encode the relationship  
 207 between flavor and mass eigenstates.

208

### 209 2.2.1.2 Quarks

210 Quarks are the basic constituents of protons and neutrons. The way quarks join to  
 211 form bound states, called “hadrons”, is through the SI. Quarks are affected by all the

---

<sup>3</sup> The weak isospin is an analogy of the isospin symmetry in strong interaction where neutron and proton are affected equally by strong force but differ in their charge.

Lepton	Q(e)	$T_3$	$L_e$	$L_\mu$	$L_\tau$	Lifetime (s)
Electron (e)	-1	-1/2	1	0	0	Stable
Electron neutrino ( $\nu_e$ )	0	1/2	1	0	0	Unknown
Muon ( $\mu$ )	-1	-1/2	0	1	0	$2.19 \times 10^{-6}$
Muon neutrino ( $\nu_\mu$ )	0	1/2	0	1	0	Unknown
Tau ( $\tau$ )	-1	-1/2	0	0	1	$290.3 \times 10^{-15}$
Tau neutrino ( $\tau_\mu$ )	0	1/2	0	0	1	Unknown

**Table 2.3:** Leptons properties [9]. Q: electric charge,  $T_3$ : weak isospin. Only left-handed leptons and right-handed anti-leptons participate in the WI. Anti-particles with inverted  $T_3$ , Q and lepton number complete the leptons set but are not listed. Right-handed leptons and left-handed anti-leptons, neither listed, form weak isospin singlets with  $T_3 = 0$  and do not take part in the weak interaction.

212 fundamental interactions which means that they carry all the four types of charges:  
 213 color, electric charge, weak isospin and mass.

Flavor	Q(e)	$I_3$	$T_3$	B	C	S	T	B'	Y	Color
Up (u)	2/3	1/2	1/2	1/3	0	0	0	0	1/3	r,b,g
Charm (c)	2/3	0	1/2	1/3	1	0	0	0	4/3	r,b,g
Top(t)	2/3	0	1/2	1/3	0	0	1	0	4/3	r,b,g
Down(d)	-1/3	-1/2	-1/2	1/3	0	0	0	0	1/3	r,b,g
Strange(s)	-1/3	0	-1/2	1/3	0	-1	0	0	-2/3	r,b,g
Bottom(b)	-1/3	0	-1/2	1/3	0	0	0	-1	-2/3	r,b,g

**Table 2.4:** Quarks properties [9]. Q: electric charge,  $I_3$ : isospin,  $T_3$ : weak isospin, B: baryon number, C: charmness, S: strangeness, T: topness, B': bottomness, Y: hypercharge. Anti-quarks posses the same mass and spin as quarks but all charges (color, flavor numbers) have opposite sign.

214

215 Table 2.4 summarizes the features of quarks, among which the most particular is  
 216 their fractional electric charge. Note that fractional charge is not a problem, given  
 217 that quarks are not found isolated, but serves to explain how composed particles are  
 218 formed out of two or more valence quarks<sup>4</sup>.

219

<sup>4</sup> Hadrons can contain an indefinite number of virtual quarks and gluons, known as the quark and gluon sea, but only the valence quarks determine hadrons' quantum numbers.



220 Color charge is the responsible for the SI between quarks and is the symmetry  
 221 ( $SU(3)_C$ ) that defines the formalism to describe SI. There are three colors: red (r),  
 222 blue(b) and green(g) and their corresponding three anti-colors; thus each quark carries  
 223 one color unit while anti-quarks carries one anti-color unit. As said above, quarks are  
 224 not allowed to be isolated due to the color confinement effect, therefore their features  
 225 have been studied indirectly by observing their bound states created when:

- 226 • one quark with a color charge is attracted by an anti-quark with the correspond-  
 227 ing anti-color charge forming a colorless particle called a “meson.”
- 228 • three quarks (anti-quarks) with different color (anti-color) charges are attracted  
 229 among them forming a colorless particle called a “baryon(anti-baryon).”

230 In the first version of the quark model (1964), M. Gell-Mann [12] and G. Zweig  
 231 [13,14] developed a consistent way to classify hadrons according to their properties.  
 232 Only three quarks (u, d, s) were involved in a scheme in which all baryons have  
 233 baryon number  $B=1$  and therefore quarks have  $B=1/3$ ; non-baryons have  $B=0$ . The  
 234 scheme organizes baryons in a two-dimensional space ( $I_3 - Y$ );  $Y$  (hypercharge) and  $I_3$   
 235 (isospin) are quantum numbers related by the Gell-Mann-Nishijima formula [15,16]:

$$Q = I_3 + \frac{Y}{2} \quad (2.2)$$

236 where  $Y = B + S + C + T + B'$  are the quantum numbers listed in table 2.4. Baryon  
 237 number is conserved in SI and EI which means that single quarks cannot be created  
 238 but in pairs  $q - \bar{q}$ .

239

240 There are six quark flavors organized in three generations (see table 2.1) following a  
 241 mass hierarchy which, again, implies that higher generations decay to first generation

quarks.

	Quarks			$T_3$	$Y_W$	Leptons			$T_3$	$Y_W$
Doublets	$\begin{pmatrix} u \\ d' \end{pmatrix}_L$	$\begin{pmatrix} c \\ s' \end{pmatrix}_L$	$\begin{pmatrix} t \\ b' \end{pmatrix}_L$	$\begin{pmatrix} 1/2 \\ -1/2 \end{pmatrix}$	1/3	$\begin{pmatrix} \nu_e \\ e \end{pmatrix}_L$	$\begin{pmatrix} \nu_\mu \\ \mu \end{pmatrix}_L$	$\begin{pmatrix} \nu_\tau \\ \tau \end{pmatrix}_L$	$\begin{pmatrix} 1/2 \\ -1/2 \end{pmatrix}$	-1
Singlets	$u_R$ $d'_R$	$c_R$ $s'_R$	$t_R$ $b'_R$	0 0	4/3 -2/3	$\nu_{eR}$ $e_R$	$\nu_{\mu R}$ $\mu_R$	$\nu_{\tau R}$ $\tau_R$	0	-2

**Table 2.5:** Fermion weak isospin and weak hypercharge multiplets. Weak hypercharge is calculated through the Gell-Mann-Nishijima formula 2.2 but using the weak isospin and charge for quarks.

Isospin doublets of quarks are also defined (see table 2.5) and as for neutrinos, the mass eigenstates are not the same as the WI eigenstates which means that members of different quark generations are connected by the WI mediator; thus, up-type quarks are coupled not to down-type quarks directly but to a superposition of down-type quarks ( $q'_d$ ) via WI according to:

$$q'_d = V_{CKM} q_d$$

$$\begin{pmatrix} d' \\ s' \\ b' \end{pmatrix} = \begin{pmatrix} V_{ud} & V_{us} & V_{ub} \\ V_{cd} & V_{cs} & V_{cb} \\ V_{td} & V_{ts} & V_{tb} \end{pmatrix} \begin{pmatrix} d \\ s \\ b \end{pmatrix} \quad (2.3)$$

where  $V_{CKM}$  is known as Cabibbo-Kobayashi-Maskawa (CKM) mixing matrix [17,18]. The weak decays of quarks are represented in the diagram of figure 2.2; again the CKM matrix plays a central role since it contains the probabilities for the different quark decay channels, in particular, note that quark decays are greatly favored between generation members.

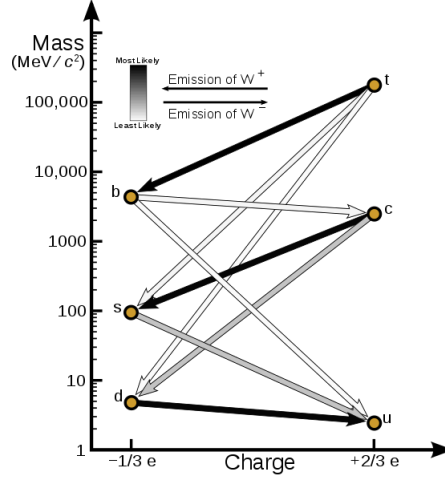


**Figure 2.2:** Transformations between quarks through the exchange of a W boson. Higher generation quarks decay to first generation quarks by emitting a W boson. The arrow color indicates the likelihood of the transition according to the grey scale in the top left side which represent the CKM matrix parameters [19].

CKM matrix is a  $3 \times 3$  unitary matrix parametrized by three mixing angles and the *CP-mixing phase*; the latter is the parameter responsible for the Charge-Parity symmetry violation (CP-violation) in the SM. The fact that the b quark decays almost all the times to a top quark is exploited in this thesis when making the selection of the signal events by requiring the presence of a jet tagged as a jet coming from a b quark in the final state. The effect of the *CP-mixing phase* on the cross section of associated production of Higgs boson and a single top process is also explored in this thesis.

## 2.2.2 Fundamental interactions

Even though there are many manifestations of force in nature, like the ones represented in figure 2.3, we can classify all of them into one of four fundamental interactions:

- *Electromagnetic interaction (EI)* affects particles that are “electrically charged,”

## Fundamental interactions.

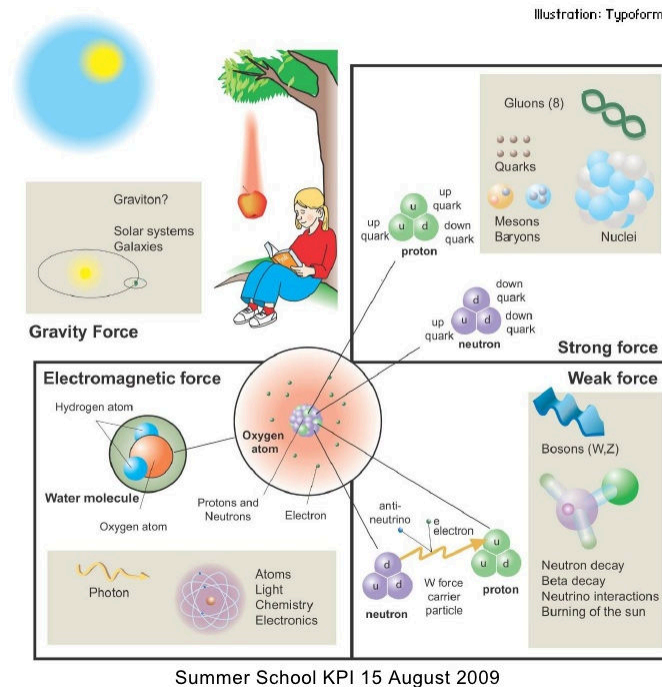


**Figure 2.3:** Fundamental interactions in nature. Despite the many manifestations of forces in nature, we can track all of them back to one of the fundamental interactions. The most common forces are gravity and electromagnetic given that all of us are subject and experience them in everyday life.

like electrons and protons. It is described by QED combining quantum mechanics, special relativity and electromagnetism in order to explain how particles with electric charge interact through the exchange of photons, therefore, one says that “Electromagnetic Force” is mediated by “photons”. Figure 2.4a. shows a graphical representation, known as “feynman diagram”, of electron-electron scattering.

- *Strong interaction (SI)* described by Quantum Chromodynamics (QCD). Hadrons like proton and neutron have internal structure given that they are composed of two or more valence quarks<sup>5</sup>. Quarks have fractional electric charge which means that they are subject to electromagnetic interaction and in the case of the

<sup>5</sup> particles made of four and five quarks are exotic states not so common.

proton they should break apart due to electrostatic repulsion; however, quarks are held together inside the hadrons against their electrostatic repulsion by the “Strong Force” through the exchange of “gluons.” The analog to the electric charge is the “color charge”. Electrons and photons are elementary particles as quarks but they don’t carry color charge, therefore they are not subject to SI. The feynnman diagram for gluon exchange between quarks is shown in figure 2.4b.

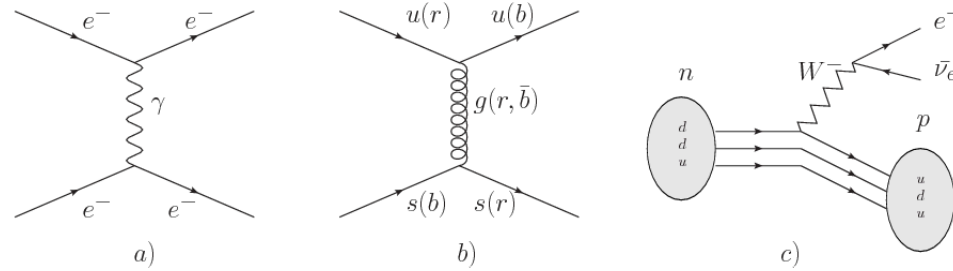


**Figure 2.4:** Feynman diagrams representing the interactions in SM; a) EI: e-e scattering; b) SI: gluon exchange between quarks ; c) WI:  $\beta$ -decay

- *Weak interaction (WI)* described by the weak theory (WT), is responsible, for instance, for the radioactive decay in atoms and proton-proton (pp) fusion within the sun. Quarks and leptons are the particles affected by the weak interaction; they possess a property called “flavor charge” (see 2.2.1) which can be changed by emitting or absorbing one weak force mediator. There are three mediators of the “weak force” known as “Z” boson in the case of electrically neutral changes and “ $W^\pm$ ” bosons in the case of electrically charged changes. The “weak isospin” is the WI analog to electric charge in EI, and color charge in SI, and defines how quarks and leptons are affected by the weak force. Figure 2.4c. shows the feynnman diagram of  $\beta$ -decay where a newutron ( $n$ ) is transformed in a proton ( $p$ ) by emmiting a  $W^-$  particle. Since this thesis is in the frame of the electroweak interaction, a more detailed description of it will be given in

298        section 2.3

299        • *Gravitational interaction (GI)* described by General Theory of Relativity (GR).  
300        It is responsible for the structure of galaxies and black holes as well as the  
301        expansion of the universe. As a classical theory, in the sense that it can be for-  
302        mulated without even appeal to the concept of quantization, it implies that the  
303        spacetime is a continuum and predictions can be made without limitation to the  
304        precision of the measurement tools. The latter represent a direct contradiction  
305        of the quantum mechanics principles. Gravity is deterministic while quantum  
306        mechanics is probabilistic; despite that, efforts to develop a quantum theory of  
307        gravity have predicted the “graviton” as mediator of the Gravitational force<sup>6</sup>.

Interaction	Acts on	Relative strength	Range (m)	Mediators
Electromagnetic (QED)	Electrically charged particles	$10^{-2}$	Infinite	Photon
Strong (QCD)	Quarks and gluons	1	$10^{-15}$	Gluon
Weak (WI)	Leptons and quarks	$10^{-6}$	$10^{-18}$	$W^{\pm}$ , Z
Gravitational (GI)	Massive particles	$10^{-39}$	Infinite	Graviton

**Table 2.6:** Fundamental interactions features [20].

308

309    Table 2.6 summarizes the main features of the fundamental interactions. The rela-  
310    tive strength of the fundamental forces reveals the meaning of strong and weak; in  
311    a context where the relative strength of the SI is 1, the EI is about hundred times  
312    weaker and WI is about million times weaker than the SI. A good description on  
313    how the relative strength and range of the fundamental interactions are calculated  
314    can be found in references [20,21]. In the everyday life, only EI and GI are explicitly  
315    experienced due to the range of these interactions; i.e., at the human scale distances

---

<sup>6</sup>    Actually a wide variety of theories have been developed in an attempt to describe gravity; some famous examples are string theory and supergravity.

only EI and GI have appreciable effects, in contrast to SI which at distances greater than  $10^{-15}\text{m}$  become negligible.

318

QED was built successfully on the basis of the classical electrodynamics theory (CED) of Maxwell and Lorentz, following theoretical and experimental requirements imposed by

- lorentz invariance: independence on the reference frame.
- locality: interacting fields are evaluated at the same space-time point to avoid action at a distance.
- renormalizability: physical predictions are finite and well defined
- particle spectrum, symmetries and conservation laws already known must emerge from the theory.
- gauge invariance.

The gauge invariance requirement reflects the fact that the fundamental fields cannot be directly measured but associated fields which are the observables. Electric (“**E**”) and magnetic (“**B**”) fields in CED are associated with the electric scalar potential “**V**” and the vector potential “**A**”. In particular, **E** can be obtained by measuring the change in the space of the scalar potential ( $\Delta V$ ); however, two scalar potentials differing by a constant “**f**” correspond to the same electric field. The same happens in the case of the vector potential “**A**”; thus, different configurations of the associated fields result in the same set of values of the observables. The freedom in choosing one particular configuration is known as “gauge freedom”; the transformation law connecting two configurations is known as “gauge transformation” and the fact that the

339 observables are not affected by a gauge transformation is called “gauge invariance”.

340

341 When the gauge tranformation:

$$\begin{aligned} \mathbf{A} &\rightarrow \mathbf{A} - \Delta f \\ V &\rightarrow V - \frac{\partial f}{\partial t} \end{aligned} \quad (2.4)$$

342 is applied to Maxwell equations, they are still satisfied and the fields remain invariant.

343 Thus, CED is invariant under gauge transformations and is called a “gauge theory”.

344 The set of all gauge transformations form the “symmetry group” of the theory, which

345 according to the group theory, has a set of “group generators”. The number of group

346 generators determine the number of “gauge fields” of the theory.

347

348 As mentioned in the first lines of section 2.2, QED has one symmetry group (U(1))

349 with one group generator (the Q operator) and one gauge field (the electromagnetic

350 field  $A^\mu$ ). In CED there is not a clear definition, beyond the historical convention, of

351 which fields are the fundamental and which are the associated, but in QED it is clear

352 that the fundamental field is  $A^\mu$ . When a gauge theory is quantized, the gauge field

353 is quantized and its quanta is called “gauge boson”. The word boson characterizes

354 particles with integer spin which obvey Bose-einstein statistics.

355

356 As will be detailed in section 2.3, interactions between partcles in a system can be

357 obtained by considering first the Lagrangian density of free particles in the system,

358 which of course is incomplete because the interaction terms have been left out, and

359 demanding global phase transformation invariance. Global phase transformation in-



variance means that a gauge transformation is performed identically to every point in the space<sup>7</sup> and the Lagrangian remains invariant. Then, the global transformation is promoted to a local phase transformation (this time the gauge transformation depends on the position in space) and again invariance is required.

364

Due to the space dependence of the local transformation, the Lagrangian density is not invariant anymore. In order to restate the gauge invariance, the gauge covariant derivative is introduced in the Lagrangian and with it the gauge field responsible for the interaction between particles in the system. The new Lagrangian density is gauge invariant, includes the interaction terms needed to account for the interactions and provides a way to explain the interaction between particles through the exchange of the gauge boson.

This recipe was used to build QED and the theories that aim to explain the fundamental interactions.

### 2.2.3 Gauge bosons

The importance of the gauge bosons comes from the fact that they are the force mediators or force carriers. The features of the gauge bosons reflect those of the fields they represent and they are extracted from the Lagrangian density used to describe the interactions. In section 2.3, it will be shown how the gauge bosons of the EI and WI emerge from the electroweak Lagrangian. The SI gauge bosons features are also extracted from the SI Lagrangian but it is not detailed in this document. The main features of the SM gauge bosons will be briefly presented below and summarized in table 2.7.

---

<sup>7</sup> Here space corresponds to the 4-dimensional space i.e. space-time.

- 383 • **Photon.** EI occurs when the photon couples to (is exchanged between) particles  
 384 carrying electric charge; however, the photon itself does not carry electric charge,  
 385 therefore, there is no coupling between photons. Given that the photon is  
 386 massless the EI is of infinite range, i.e., electrically charged particles interact  
 387 even if they are located far away one from each other; this also implies that  
 388 photons always move with the speed of light.
- 389 • **Gluon.** SI is mediated by gluons which, same as photons, are massless. They  
 390 carry one unit of color charge and one unit of anticolor charge which means that  
 391 gluons couple to other gluons. As a result, the range of the SI is not infinite  
 392 but very short due to the attraction between gluons, giving rise to the “color  
 393 confinement” which explains why color charged particles cannot be isolated but  
 394 live within composited particles, like quarks inside protons.
- 395 • **W, Z.** The WI mediators,  $W^\pm$  and Z, are massive which explains their short-  
 396 range. Given that the WI is the only interaction that can change the flavor  
 397 of the interacting particles, the W boson is the responsible for the nuclear  
 398 transmutation where a neutron is converted in a proton or vice versa with the  
 399 involvement of an electron and a neutrino (see figure 2.4c). The Z boson is the  
 400 responsible of the neutral weak processes like neutrino elastic scattering where  
 401 no electric charge but momentum transference is involved. WI gauge bosons  
 402 carry isospin charge which makes posible the interaction between them.

Interaction	Mediator	Electric charge (e)	Color charge	Weak Isospin	mass (GeV/c <sup>2</sup> )
Electromagnetic	Photon ( $\gamma$ )	0	No	0	0
Strong	Gluon (g)	0	Yes -octet	No	0
Weak	$W^\pm$	$\pm 1$	No	$\pm 1$	$80.385 \pm 0.015$
	Z	0	No	0	$91.188 \pm 0.002$

**Table 2.7:** SM gauge bosons main features [9].

## 404   **2.3   Electroweak unification and the Higgs**

### 405   **mechanism**

406   Physicists dream of building a theory that contains all the interactions in one single  
 407   interaction, i.e., showing that at some scale in energy all the four fundamental in-  
 408   teractions are unified and only one interaction emerges in a “Theory of everything”.  
 409   The first sign of the feasibility of such unification comes from success in the con-  
 410   struction of the CED. Einstein spent years trying to reach that dream, which by  
 411   1920 only involved electromagnetism and gravity, with no success; however, a new  
 412   partial unification was achieved in the 1960’s, when S.Glashow [22], A.Salam [23] and  
 413   S.Weinberg [24] independently proposed that electromagnetic and weak interactions  
 414   are two manifestations of a more general interaction called “electroweak interaction  
 415   (EWT)”. Both, QCD and EWT, were developed in parallel and following the useful  
 416   prescription provided by QED and the gauge invariance principles.

417

418   The theory of weak interactions was capable of explaining the  $\beta$ -decay and in general  
 419   the processes mediated by  $W^\pm$  bosons. However, there were some processes like the  
 420   “ $\nu_\mu - e$  scattering” which would require the exchange of two W bosons (see figure 2.5  
 421   top diagrams) giving rise to divergent loop integrals and then non finite predictions.  
 422   By including neutral currents involving fermions via the exchange of neutral bosons  
 423   Z, those divergences are compensated and the predictions become realistic.

424

425   Neutral weak interaction vertices conserve flavor in the same way as the electromag-  
 426   netic vertices do, but additionally, the Z boson can couple to neutrinos which implies  
 427   that processes involving charged fermions can proceed through EI or WI but processes  
 428   involving neutrinos can proceed only through WI.

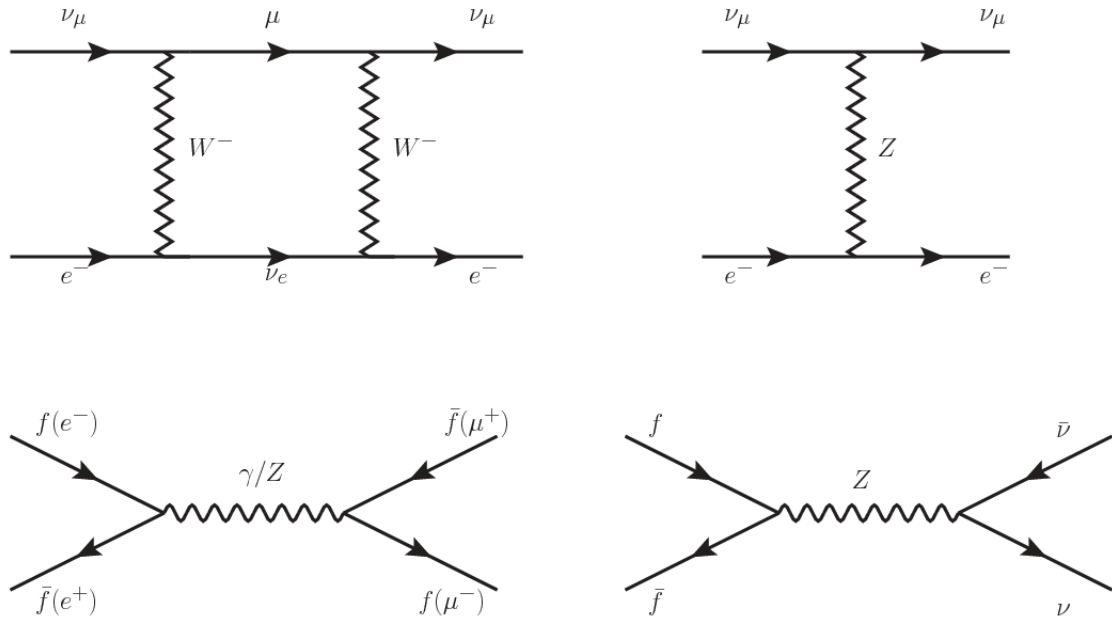


**Figure 2.5:** Top:  $\nu_\mu - e^-$  scattering going through charged currents (left) and neutral currents (right). Bottom: neutral current processes for charged fermions (left) and involving neutrinos (right). While neutral current processes involving only charged fermions can proceed through EI or WI, those involving neutrinos can only proceed via WI.

429

430 The prescription to build a gauge theory of the WI consists of proposing a free field  
 431 Lagrangian density that includes the particles involved; next, by requesting invari-  
 432 ance under global phase transformations first and generalizing to local phase trans-  
 433 formations invariance later, the conserved currents are identified and interactions are  
 434 generated by introducing gauge fields. Given that the goal is to include the EI and  
 435 WI in a single theory, the group symmetry considered should be a combination of  
 436  $SU(2)_L$  and  $U(1)_{em}$ , however the latter cannot be used directly because the EI treats  
 437 left and right-handed particles indistinctly in contrast to the former. Fortunately, the  
 438 weak hypercharge, which is a combination of the weak isospin and the electric charge  
 439 (eqn 2.2) is suitable to be used since it is conserved by the EI and WI. Thus, the  
 440 symmetry group to be considered is

$$G \equiv SU(2)_L \otimes U(1)_Y \quad (2.5)$$

441 The following treatment applies to any of the fermion generations, but for simplicity  
 442 the first generation of leptons will be considered [5, 6, 25, 26].

443

444 Given the first generation of leptons

$$\psi_1 = \begin{pmatrix} \nu_e \\ e^- \end{pmatrix}_L, \quad \psi_2 = \nu_{eR}, \quad \psi_3 = e_R^- \quad (2.6)$$

445 the charged fermionic currents are given by

$$J_\mu \equiv J_\mu^+ = \bar{\nu}_{eL} \gamma_\mu e_L, \quad J_\mu^\dagger \equiv J_\mu^- = \bar{e}_L \gamma_\mu \nu_{eL} \quad (2.7)$$

446 and the free Lagrangian is given by

$$\mathcal{L}_0 = \sum_{j=1}^3 i \bar{\psi}_j(x) \gamma^\mu \partial_\mu \psi_j(x). \quad (2.8)$$

447 Mass terms are included directly in the QED and QCD free Lagrangians since they  
 448 preserve the invariance under the symmetry transformations involved which treat  
 449 left-handed and right-handed similarly, however mass terms of the form

$$m_W^2 W_\mu^\dagger(x) W^\mu(x) + \frac{1}{2} m_Z^2 Z_\mu(x) Z^\mu(x) - m_e \bar{\psi}_e(x) \psi_e(x) \quad (2.9)$$

450 which represent the mass of  $W^\pm$ , Z and electrons, are not invariant under G trans-  
 451 formations, therefore the gauge fields described by the EWI are in principle massless.

452

453 Experiments have shown that the gauge fields are not massless; however, they have

454 to acquire mass through a mechanism compatible with the gauge invariance; that  
 455 mechanism is known as the “Higgs mechanism” and will be considered later in this  
 456 section. The global transformations in the combined symmetry group  $G$  can be  
 457 written as

$$\begin{aligned}
 \psi_1(x) &\xrightarrow{G} \psi'_1(x) \equiv U_Y U_L \psi_1(x), \\
 \psi_2(x) &\xrightarrow{G} \psi'_2(x) \equiv U_Y \psi_2(x), \\
 \psi_3(x) &\xrightarrow{G} \psi'_3(x) \equiv U_Y \psi_3(x)
 \end{aligned}
 \tag{2.10}$$

458 where  $U_L$  represent the  $SU(2)_L$  transformation acting only on the weak isospin dou-  
 459 blet and  $U_Y$  represent the  $U(1)_Y$  transformation acting on all the weak isospin mul-  
 460 tiplets. Explicitly

$$U_L \equiv \exp\left(i\frac{\sigma_i}{2}\alpha^i\right), \quad U_Y \equiv \exp(iy_i\beta) \quad (i = 1, 2, 3) \tag{2.11}$$

461 with  $\sigma_i$  the Pauli matrices and  $y_i$  the weak hypercharges. In order to promote the  
 462 transformations from global to local while keeping the invariance, it is required that  
 463  $\alpha^i = \alpha^i(x)$ ,  $\beta = \beta(x)$  and the replacement of the ordinary derivatives by the covariant  
 464 derivatives

$$\begin{aligned}
 D_\mu \psi_1(x) &\equiv \left[ \partial_\mu + ig\sigma_i W_\mu^i(x)/2 + ig'y_1 B_\mu(x) \right] \psi_1(x) \\
 D_\mu \psi_2(x) &\equiv \left[ \partial_\mu + ig'y_2 B_\mu(x) \right] \psi_2(x) \\
 D_\mu \psi_3(x) &\equiv \left[ \partial_\mu + ig'y_3 B_\mu(x) \right] \psi_3(x)
 \end{aligned}
 \tag{2.12}$$

introducing in this way four gauge fields,  $W_\mu^i(x)$  and  $B_\mu(x)$ , in the process. The covariant derivatives (eqn 2.12) are required to transform in the same way as fermion fields  $\psi_i(x)$  themselves, therefore, the gauge fields transform as:

$$\begin{aligned} B_\mu(x) &\xrightarrow{G} B'_\mu(x) \equiv B_\mu(x) - \frac{1}{g'} \partial_\mu \beta(x) \\ W_\mu^i(x) &\xrightarrow{G} W_\mu^{i'}(x) \equiv W_\mu^i(x) - \frac{i}{g} \partial_\mu \alpha_i(x) - \varepsilon_{ijk} \alpha_j(x) W_\mu^k(x). \end{aligned} \quad (2.13)$$

The G invariant version of the Lagrangian density 2.8 can be written as

$$\mathcal{L}_0 = \sum_{j=1}^3 i \bar{\psi}_j(x) \gamma^\mu D_\mu \psi_j(x) \quad (2.14)$$

where free massless fermion and gauge fields and fermion-gauge boson interactions are included. The EWI Lagrangian density must additionally include kinetic terms for the gauge fields ( $\mathcal{L}_G$ ) which are built from the field strengths, according to

$$B_{\mu\nu}(x) \equiv \partial_\mu B_\nu - \partial_\nu B_\mu \quad (2.15)$$

$$W_{\mu\nu}^i(x) \equiv \partial_\mu W_\nu^i(x) - \partial_\nu W_\mu^i(x) - g \varepsilon^{ijk} W_\mu^j W_\nu^k \quad (2.16)$$

the last term in eqn. 2.16 is added in order to hold the gauge invariance; therefore,

$$\mathcal{L}_G = -\frac{1}{4} B_{\mu\nu}(x) B^{\mu\nu}(x) - \frac{1}{4} W_{\mu\nu}^i(x) W_i^{\mu\nu}(x) \quad (2.17)$$

which contains not only the free gauge fields contributions, but also the gauge fields self-interactions and interactions among them.

476 The three weak isospin conserved currents resulting from the  $SU(2)_L$  symmetry are  
 477 given by

$$J_\mu^i(x) = \frac{1}{2} \bar{\psi}_1(x) \gamma_\mu \sigma^i \psi_1(x) \quad (2.18)$$

478 while the weak hypercharge conserved current resulting from the  $U(1)_Y$  symmetry is  
 479 given by

$$J_\mu^Y = \sum_{j=1}^3 \bar{\psi}_j(x) \gamma_\mu y_j \psi_j(x) \quad (2.19)$$

480 In order to evaluate the electroweak interactions modeled by an isotriplet field  $W_\mu^i$   
 481 which couples to isospin currents  $J_\mu^i$  with strength  $g$  and additionally the singlet  
 482 field  $B_\mu$  which couples to the weak hypercharge current  $J_\mu^Y$  with strength  $g'/2$ . The  
 483 interaction Lagrangian density to be considered is

$$\mathcal{L}_I = -g J^{i\mu}(x) W_\mu^i(x) - \frac{g'}{2} J^{Y\mu}(x) B_\mu(x) \quad (2.20)$$

484 Note that the weak isospin currents are not the same as the charged fermionic currents  
 485 that were used to describe the WI (eqn 2.7), since the weak isospin eigenstates are  
 486 not the same as the mass eigenstates, but they are closely related

$$J_\mu = \frac{1}{2} (J_\mu^1 + i J_\mu^2), \quad J_\mu^\dagger = \frac{1}{2} (J_\mu^1 - i J_\mu^2). \quad (2.21)$$

487 The same happens with the gauge fields  $W_\mu^i$  which are related to the mass eigenstates  
 488  $W^\pm$  by

$$W_\mu^+ = \frac{1}{\sqrt{2}} (W_\mu^1 - i W_\mu^2), \quad W_\mu^- = \frac{1}{\sqrt{2}} (W_\mu^1 + i W_\mu^2). \quad (2.22)$$



489 The fact that there are three weak isospin conserved currents is an indication that in  
 490 addition to the charged fermionic currents, which couple charged to neutral leptons,  
 491 there should be a neutral fermionic current that does not involve electric charge  
 492 exchange; therefore, it couples neutral fermions or fermions of the same electric charge.  
 493 The third weak isospin current contains a term that is similar to the electromagnetic  
 494 current ( $j_\mu^{em}$ ), indicating that there is a relation between them and resembling the  
 495 Gell-Mann-Nishijima formula 2.2 adapted to electroweak interactions

$$Q = T_3 + \frac{Y_W}{2}. \quad (2.23)$$

496 Just as  $Q$  generates the  $U(1)_{em}$  symmetry, the weak hypercharge generates the  $U(1)_Y$   
 497 symmetry as said before. It is possible to write the relationship in terms of the currents  
 498 as

$$j_\mu^{em} = J_\mu^3 + \frac{1}{2} J_\mu^Y. \quad (2.24)$$

499 The neutral gauge fields  $W_\mu^3$  and  $B_\mu$  cannot be directly identified with the  $Z$  and the  
 500 photon fields since the photon interacts similarly with left and right-handed fermions;  
 501 however, they are related through a linear combination given by

$$\begin{aligned} A_\mu &= B_\mu \cos \theta_W + W_\mu^3 \sin \theta_W \\ Z_\mu &= -B_\mu \sin \theta_W + W_\mu^3 \cos \theta_W \end{aligned} \quad (2.25)$$

502 where  $\theta_W$  is known as the “Weinberg angle.” The interaction Lagrangian is now given

503 by

$$\mathcal{L}_I = -\frac{g}{\sqrt{2}}(J^\mu W_\mu^+ + J^{\mu\dagger} W_\mu^-) - \left(g \sin \theta_W J_\mu^3 + g' \cos \theta_W \frac{J_\mu^Y}{2}\right) A^\mu - \left(g \cos \theta_W J_\mu^3 - g' \sin \theta_W \frac{J_\mu^Y}{2}\right) Z^\mu \quad (2.26)$$

504 the first term is the weak charged current interaction, while the second term is the  
505 electromagnetic interaction under the condition

$$g \sin \theta_W = g' \cos \theta_W = e, \quad \frac{g'}{g} = \tan \theta_W \quad (2.27)$$

506 contained in the eqn.2.24; the third term is the neutral weak current.

507

508 Note that the neutral fields transformation given by the eqn. 2.25 can be written in  
509 terms of the coupling constants  $g$  and  $g'$  as:

$$A_\mu = \frac{g' W_\mu^3 + g B_\mu}{\sqrt{g^2 + g'^2}}, \quad Z_\mu = \frac{g W_\mu^3 - g' B_\mu}{\sqrt{g^2 + g'^2}} \quad (2.28)$$

510 So far, the Lagrangian density describing the non-massive EWI is:

$$\mathcal{L}_{nmEWI} = \mathcal{L}_0 + \mathcal{L}_G \quad (2.29)$$

511 where fermion and gauge fields have been considered massless because their regular  
512 mass terms are manifestly non invariant under G transformations; therefore, masses  
513 have to be generated in a gauge invariant way. The mechanism by which this goal is  
514 achieved is known as the “Higgs mechanism” and is closely connected to the concept  
515 of “spontaneous symmetry breaking.”

### 516 2.3.1 Spontaneous symmetry breaking (SSB)

517 Figure 2.6 left shows a steel nail (top) which is subject to an external force; the form  
 518 of the potential energy is also shown (bottom).

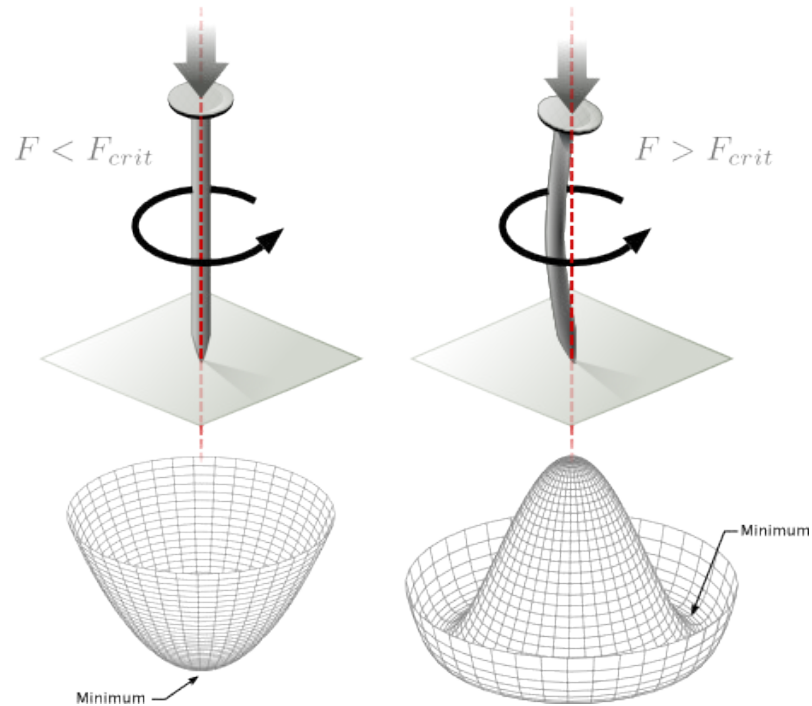


**Figure 2.6:** Spontaneous symmetry breaking mechanism. The steel nail, subject to an external force (top left), has rotational symmetry with respect to its axis. When the external force overcomes a critical value the nail buckles (top right) choosing a minimal energy state (ground state) and thus “*breaking spontaneously the rotational symmetry*”. The potential energy (bottom) changes but holds the rotational symmetry; however, an infinite number of asymmetric ground states are generated and circularly distributed in the bottom of the potential [27].

519

520 Before reaching the critical force value, the system has rotational symmetry with re-  
 521 spect to the nail axis; however, after the critical force value is reached the nail buckles  
 522 (top right). The form of the potential energy (bottom right) changes, preserving its  
 523 rotational symmetry although its minima does not exhibit that rotational symmetry  
 524 any longer. Right before the nail buckles there is no indication of the direction the

525 nail will bend because any of the directions are equivalent, but once the nail bends,  
 526 choosing a direction, an arbitrary minimal energy state (ground state) is selected and  
 527 it does not share the system's rotational symmetry. This mechanism for reaching an  
 528 asymmetric ground state is known as “*spontaneous symmetry breaking*”.

529 The lesson from this analysis is that the way to introduce the SSB mechanism into a  
 530 system is by adding the appropriate potential to it.

531

532 Figure 2.7 shows a plot of the potential  $V(\phi)$  in the case of a scalar field  $\phi$

$$V(\phi) = \mu^2 \phi^\dagger \phi + \lambda (\phi^\dagger \phi)^2 \quad (2.30)$$

533 If  $\mu^2 > 0$  the potential has only one minimum at  $\phi = 0$  and describes a scalar field  
 534 with mass  $\mu$ . If  $\mu^2 < 0$  the potential has a local maximum at  $\phi = 0$  and two minima  
 535 at  $\phi = \pm \sqrt{-\mu^2/\lambda}$  which enables the SSB mechanism to work.

536

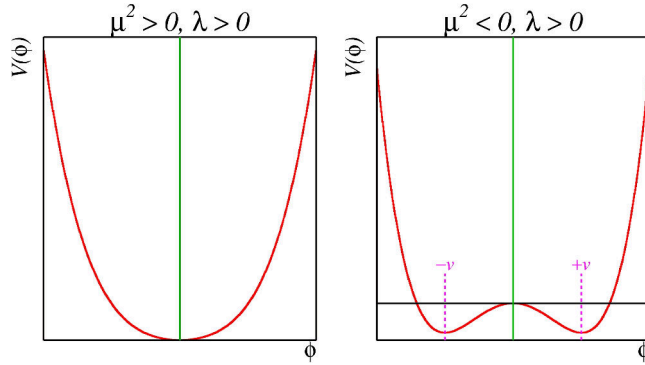


**Figure 2.7:** Shape of the potential  $V(\phi)$  for  $\lambda > 0$  and:  $\mu^2 > 0$  (left) and  $\mu^2 < 0$  (right). The case  $\mu^2 < 0$  corresponds to the potential suitable for introducing the SSB mechanism by choosing one of the two ground states which are connected via reflection symmetry. [27].

537 In the case of a complex scalar field  $\phi(x)$

$$\phi(x) = \frac{1}{\sqrt{2}}(\phi_1 + i\phi_2) \quad (2.31)$$

538 the Lagrangian (invariant under global  $U(1)$  transformations) is given by

$$\mathcal{L} = (\partial_\mu \phi)^\dagger (\partial^\mu \phi) - V(\phi), \quad V(\phi) = \mu^2 \phi^\dagger \phi + \lambda (\phi^\dagger \phi)^2 \quad (2.32)$$

539 where an appropriate potential has been added in order to introduce the SSB.

540

541 As seen in figure 2.8, the potential has now an infinite number of minima circularly  
 542 distributed along the  $\xi$ -direction which makes possible the occurrence of the SSB by  
 543 choosing an arbitrary ground state; for instance,  $\xi = 0$ , i.e.  $\phi_1 = v, \phi_2 = 0$

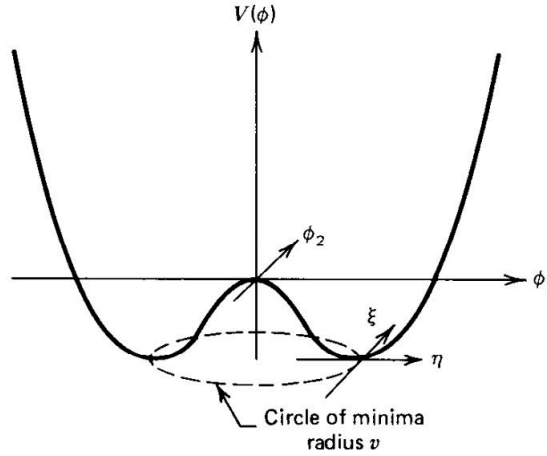


**Figure 2.8:** Potential for complex scalar field. There is a circle of minima of radius  $v$  along the  $\xi$ -direction [6].

$$\phi_0 = \frac{v}{\sqrt{2}} \exp(i\xi) \xrightarrow{SSB} \phi_0 = \frac{v}{\sqrt{2}} \quad (2.33)$$

544 As usual, excitations over the ground state are studied by making an expansion about

545 it; thus, the excitation can be parametrized as:

$$\phi(x) = \frac{1}{\sqrt{2}}(v + \eta(x) + i\xi(x)) \quad (2.34)$$

546 which when substituted into eqn. 2.32 produces a Lagrangian in terms of the new  
547 fields  $\eta$  and  $\xi$

$$\mathcal{L}' = \frac{1}{2}(\partial_\mu \xi)^2 + \frac{1}{2}(\partial_\mu \eta)^2 + \mu^2 \eta^2 - V(\phi_0) - \lambda v \eta(\eta^2 + \xi^2) - \frac{\lambda}{4}(\eta^2 + \xi^2)^2 \quad (2.35)$$

548 where the last two terms represent the interactions and self-interaction between the  
549 two fields  $\eta$  and  $\xi$ . The particular feature of the SSB mechanism is revealed when  
550 looking to the first three terms of  $\mathcal{L}'$ . Before the SSB, only the massless  $\phi$  field is  
551 present in the system; after the SSB there are two fields of which the  $\eta$ -field has  
552 acquired mass  $m_\eta = \sqrt{-2\mu^2}$  while the  $\xi$ -field is still massless (see figure 2.9).

553

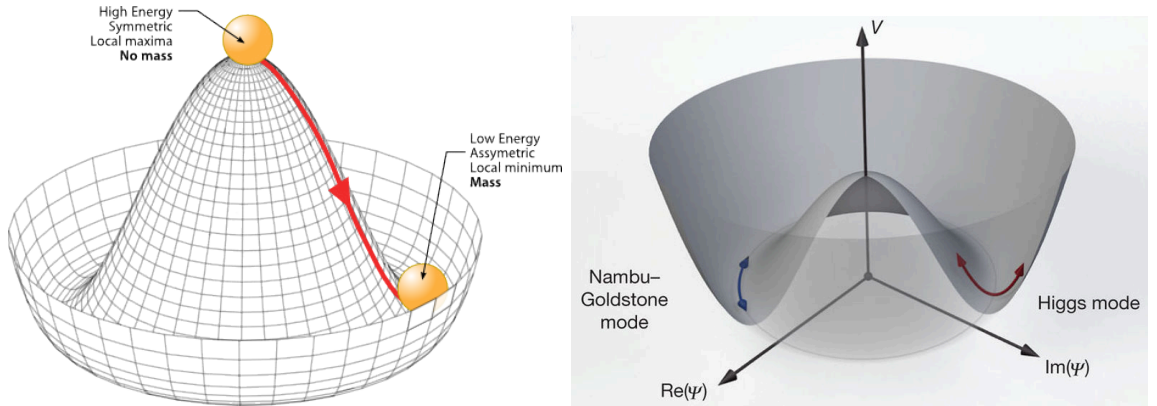


**Figure 2.9:** SSB mechanism for a complex scalar field [27, 28].

554 Thus, the SSB mechanism serves as a method to generate mass but as a side effect a  
555 massless field is introduced in the system. This fact is known as the Goldstone theorem

and states that a massless scalar field appears in the system for each continuous symmetry spontaneously broken. Another version of the Goldstone theorem states that “if a Lagrangian is invariant under a continuous symmetry group  $G$ , but the vacuum is only invariant under a subgroup  $H \subset G$ , then there must exist as many massless spin-0 particles (Nambu-Goldstone bosons) as broken generators.” [26] The Nambu-Goldstone boson can be understood considering that the potential in the  $\xi$ -direction is flat so excitations in that direction are not energy consuming and thus represent a massless state.

### 2.3.2 Higgs mechanism

When the SSB mechanism is introduced in the formulation of the EWI in an attempt to generate the mass of the so far massless gauge bosons and fermions, an interesting effect is revealed. In order to keep the  $G$  symmetry group invariance and generate the mass of the EW gauge bosons, a  $G$  invariant Lagrangian density ( $\mathcal{L}_S$ ) has to be added to the non massive EWI Lagrangian (eqn. 2.29)

$$\mathcal{L}_S = (D_\mu \phi)^\dagger (D^\mu \phi) - \mu^2 \phi^\dagger \phi - \lambda (\phi^\dagger \phi)^2, \quad \lambda > 0, \mu^2 < 0 \quad (2.36)$$

$$D_\mu \phi = \left( i\partial_\mu - g \frac{\sigma_i}{2} W_\mu^i - g' \frac{Y}{2} B_\mu \right) \phi \quad (2.37)$$

$\phi$  has to be an isospin doublet of complex scalar fields so it preserves the  $G$  invariance; thus  $\phi$  can be defined as:

$$\phi = \begin{pmatrix} \phi^+ \\ \phi^0 \end{pmatrix} \equiv \frac{1}{\sqrt{2}} \begin{pmatrix} \phi_1 + i\phi_2 \\ \phi_3 + i\phi_4 \end{pmatrix}. \quad (2.38)$$

The minima of the potential are defined by

$$\phi^\dagger \phi = \frac{1}{2}(\phi_1^2 + \phi_2^2 + \phi_3^2 + \phi_4^2) = -\frac{\mu^2}{2\lambda}. \quad (2.39)$$

573 The choice of the ground state is critical. By choosing a ground state, invariant under  
 574  $U(1)_{em}$  gauge symmetry, the photon will remain massless and the  $W^\pm$  and  $Z$  bosons  
 575 masses will be generated which is exactly what is needed. In that sense, the best  
 576 choice corresponds to a weak isospin doublet with  $T_3 = -1/2$ ,  $Y_W = 1$  and  $Q = 0$   
 577 which defines a ground state with  $\phi_1 = \phi_2 = \phi_4$  and  $\phi_3 = v$ :

$$\phi_0 \equiv \frac{1}{\sqrt{2}} \begin{pmatrix} 0 \\ v \end{pmatrix}, \quad v^2 \equiv -\frac{\mu^2}{\lambda}. \quad (2.40)$$

578 where the vacuum expectation value  $v$  is fixed by the Fermi coupling  $G_F$  according  
 579 to  $v = (\sqrt{2}G_F)^{1/2} \approx 246$  GeV.

580

581 The G symmetry has been broken and three Nambu-Goldstone bosons will appear.  
 582 The next step is to expand  $\phi$  about the chosen ground state as:

$$\phi(x) = \frac{1}{\sqrt{2}} \exp\left(\frac{i}{v} \sigma_i \theta^i(x)\right) \begin{pmatrix} 0 \\ v + H(x) \end{pmatrix} \approx \frac{1}{\sqrt{2}} \begin{pmatrix} \theta_1(x) + i\theta_2(x) \\ v + H(x) - i\theta_3(x) \end{pmatrix} \quad (2.41)$$

583 to describe fluctuations from the ground state  $\phi_0$ . The fields  $\theta_i(x)$  represent the  
 584 Nambu-Goldstone bosons while  $H(x)$  is known as “higgs field.” The fundamental  
 585 feature of the parametrization used is that the dependence on the  $\theta_i(x)$  fields is  
 586 factored out in a global phase that can be eliminated by taking the physical “unitary  
 587 gauge”  $\theta_i(x) = 0$ . Therefore the expansion about the ground state is given by:

$$\phi(x) \frac{1}{\sqrt{2}} \begin{pmatrix} 0 \\ v + H(x) \end{pmatrix} \quad (2.42)$$



588 which when substituted into  $\mathcal{L}_S$  (eqn. 2.36) results in a Lagrangian containing the now  
 589 massive three gauge bosons  $W^\pm, Z$ , one massless gauge boson (photon) and the new  
 590 Higgs field (H). The three degrees of freedom corresponding to the Nambu-Goldstone  
 591 bosons are now integrated into the massive gauge bosons as their longitudinal po-  
 592 larizations which were not available when they were massless particles. The effect  
 593 by which vector boson fields acquire mass after an spontaneous symmetry breaking,  
 594 but without an explicit gauge invariance breaking is known as the “*Higgs mechanism*”.

595

596 The mechanism was proposed by three independent groups: F.Englert and R.Brout  
 597 in August 1964 [29], P.Higgs in October 1964 [30] and G.Guralnik, C.Hagen and  
 598 T.Kibble in November 1964 [31]; however, its importance was not realized until  
 599 S.Glashow [22], A.Salam [23] and S.Weinberg [24], independently, proposed that elec-  
 600 tromagnetic and weak interactions are two manifestations of a more general interac-  
 601 tion called “electroweak interaction” in 1967.

### 602 2.3.3 Masses of the gauge bosons

603 The mass of the gauge bosons is extracted by evaluating the kinetic part of Lagrangian  
 604  $\mathcal{L}_S$  in the ground state (known also as the vacuum expectation value), i.e.,

$$\left| \left( \partial_\mu - ig \frac{\sigma_i}{2} W_\mu^i - i \frac{g'}{2} B_\mu \right) \phi_0 \right|^2 = \left( \frac{1}{2} v g \right)^2 W_\mu^+ W^{-\mu} + \frac{1}{8} v^2 (W_\mu^3, B_\mu) \begin{pmatrix} g^2 & -gg' \\ -gg' & g'^2 \end{pmatrix} \begin{pmatrix} W^{3\mu} \\ B^\mu \end{pmatrix} \quad (2.43)$$

605 comparing with the typical mass term for a charged boson  $M_W^2 W^+ W^-$

$$M_W = \frac{1}{2} v g. \quad (2.44)$$

The second term in the right side of the eqn.2.43 comprises the masses of the neutral

bosons, but it needs to be written in terms of the gauge fields  $Z_\mu$  and  $A_\mu$  in order to be compared to the typical mass terms for neutral bosons, therefore using eqn. 2.28

$$\begin{aligned} \frac{1}{8}v^2[g^2(W_\mu^3)^2 - 2gg'W_\mu^3B^\mu + g'^2B_\mu^2] &= \frac{1}{8}v^2[gW_\mu^3 - g'B_\mu]^2 + 0[g'W_\mu^3 + gB_\mu]^2 \\ &= \frac{1}{8}v^2[\sqrt{g^2 + g'^2}Z_\mu]^2 + 0[\sqrt{g^2 + g'^2}A_\mu]^2 \end{aligned} \quad (2.45)$$

and then

$$M_Z = \frac{1}{2}v\sqrt{g^2 + g'^2}, \quad M_A = 0 \quad (2.46)$$

### 2.3.4 Masses of the fermions

The lepton mass terms can be generated by introducing a gauge invariant Lagrangian term describing the Yukawa coupling between the lepton field and the Higgs field

$$\mathcal{L}_{Yl} = -G_l \left[ (\bar{\nu}_l, \bar{l})_L \begin{pmatrix} \phi^+ \\ \phi^0 \end{pmatrix} l_R + \bar{l}_R (\phi^-, \bar{\phi}^0) \begin{pmatrix} \nu_l \\ l \end{pmatrix}_L \right], \quad l = e, \mu, \tau. \quad (2.47)$$

After the SSB and replacing the usual field expansion about the ground state (eqn.2.40) into  $\mathcal{L}_{Yl}$ , the mass term arises

$$\mathcal{L}_{Yl} = -m_l(\bar{l}_L l_R + \bar{l}_R l_L) - \frac{m_l}{v}(\bar{l}_L l_R + \bar{l}_R l_L)H = -m_l \bar{l}l \left(1 + \frac{H}{v}\right) \quad (2.48)$$

612

$$m_l = \frac{G_l}{\sqrt{2}}v \quad (2.49)$$

where the additional term represents the lepton-Higgs interaction. The quark masses are generated in a similar way as lepton masses but for the upper member of the

quark doublet a different Higgs doublet is needed:

$$\phi_c = -i\sigma_2\phi^* = \begin{pmatrix} -\bar{\phi}^0 \\ \phi^- \end{pmatrix}. \quad (2.50)$$

Additionally, given that the quark isospin doublets are not constructed in terms of the mass eigenstates but in terms of the flavor eigenstates, as shown in table 2.5, the coupling parameters will be related to the CKM matrix elements; thus the quark Lagrangian is given by:

$$\mathcal{L}_{Yq} = -G_d^{i,j}(\bar{u}_i, \bar{d}'_i)_L \begin{pmatrix} \phi^+ \\ \phi^0 \end{pmatrix} d_{jR} - G_u^{i,j}(\bar{u}_i, \bar{d}'_i)_L \begin{pmatrix} -\bar{\phi}^0 \\ \phi^- \end{pmatrix} u_{jR} + h.c. \quad (2.51)$$

with  $i,j=1,2,3$ . After SSB and expansion about the ground state, the diagonal form of  $\mathcal{L}_{Yq}$  is:

$$\mathcal{L}_{Yq} = -m_d^i \bar{d}_i d_i \left(1 + \frac{H}{v}\right) - m_u^i \bar{u}_i u_i \left(1 + \frac{H}{v}\right) \quad (2.52)$$

Fermion masses depend on arbitrary couplings  $G_l$  and  $G_{u,d}$  and are not predicted by the theory.

### 2.3.5 The Higgs field

After the characterization of the fermions and gauge bosons as well as their interactions, it is necessary to characterize the Higgs field itself. The Lagrangian  $\mathcal{L}_S$  in eqn. 2.36 written in terms of the gauge bosons is given by

$$\mathcal{L}_S = \frac{1}{4}\lambda v^4 + \mathcal{L}_H + \mathcal{L}_{HV} \quad (2.53)$$

$$\mathcal{L}_H = \frac{1}{2}\partial_\mu H \partial^\mu H - \frac{1}{2}m_H^2 H^2 - \frac{1}{2v}m_H^2 H^3 - \frac{1}{8v^2}m_H^2 H^4 \quad (2.54)$$

$$\mathcal{L}_{HV} = m_H^2 W_\mu^+ W^{\mu-} \left(1 + \frac{2}{v}H + \frac{2}{v^2}H^2\right) + \frac{1}{2}m_Z^2 Z_\mu Z^\mu \left(1 + \frac{2}{v}H + \frac{2}{v^2}H^2\right) \quad (2.55)$$

630 The mass of the Higgs boson is deduced as usual from the mass term in the Lagrangian  
631 resulting in:

$$m_H = \sqrt{-2\mu^2} = \sqrt{2\lambda}v \tag{2.56}$$

632 however, it is not predicted by the theory either. The experimental efforts to find  
633 the Higgs boson, carried out by the “Compact Muon Solenoid (CMS)” experiment  
634 and the “A Toroidal LHC Apparatus (ATLAS)” experiments at the “Large Hadron  
635 Collider(LHC)”, gave great results by July of 2012 when the discovery of a new  
636 particle compatible with the Higgs boson predicted by the electroweak theory [32,33]  
637 was announced. Although at the announcement time there were some reservations  
638 about calling the new particle the “Higgs boson”, today this name is widely accepted.  
639 The Higgs mass measurement, reported by both experiments [34], is in table 2.8.

Property	Value
Electric charge	0
Colour charge	0
Spin	0
Weak isospin	-1/2
Weak hypercharge	1
Parity	1
Mass (GeV/c <sup>2</sup> )	125.09±0.21 (stat.)±0.11 (syst.)

**Table 2.8:** Higgs boson properties. Higgs mass is not predicted by the theory and the value here corresponds to the experimental measurement.

640

641 **2.3.6 Production of Higgs bosons at LHC**

642 At LHC, Higgs boson is produced as a result of the collision of two counter-rotating  
643 protons beams. A detailed description of the LHC machine will be presented in  
644 chapter ???. “The total cross section” is a parameter that quantifies the number of  
645 pp collisions that happen when a number of protons are fired at each other. Different  
646 results can be obtained after a pp collision and for each one the “cross section” is

647 defined as the number of pp collisions that conclude in that particular result with  
 648 respect to the number of protons fired at each other.

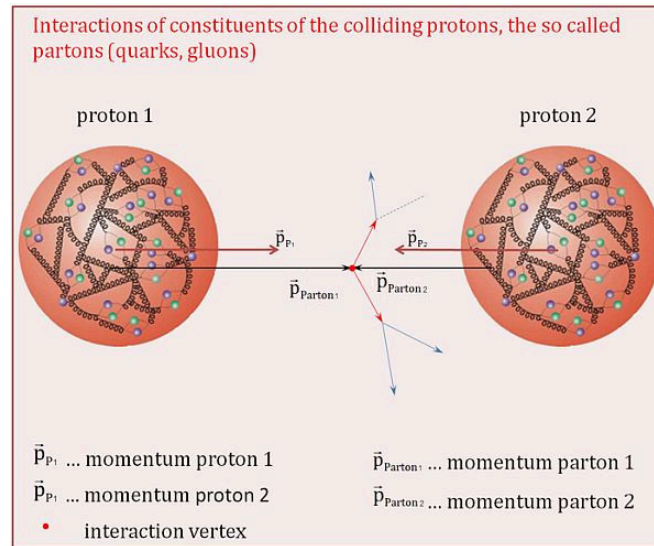


**Figure 2.10:** Proton-proton collision. Protons are composed of 3 valence quarks, a sea of quarks and gluons; therefore in a proton-proton collision, quarks and gluons are those who collide. [35].

648

649 Protons are composed of quarks and these quarks are bound by gluons; however,  
 650 what is commonly called the quark content of the proton makes reference to the  
 651 valence quarks. A sea of quarks and gluons is also present inside the proton as repre-  
 652 sented in figure 2.10. In a proton-proton (pp) collision, the constituents (quarks and  
 653 gluons) are those who collide. The pp cross section depends on the momentum of  
 654 the colliding particles, reason for which it is needed to know how the momentum is  
 655 distributed inside the proton. Quarks and gluons are known as partons and the func-  
 656 tions that describe how the proton momentum is distributed among partons inside it  
 657 are called “parton distribution functions (PDFs)”;

658 PDFs are determined from experi-  
 659 mental data obtained in experiments where the internal structure of hadrons is tested.

659

660 In addition, in physics, a common approach to study complex systems consists in

starting with a simpler version of them, for which a well known description is available, and add an additional “perturbation” which represents a small deviation from the known behavior. If the perturbation is small enough, the physical quantities associated with the perturbed system are expressed as a series of corrections to those of the simpler system; therefore, the more terms are considered in the series (the higher order in the perturbation series), the more precise is the the description of the complex system.

668

This thesis explores the Higgs production at LHC; therefore the overview presented here will be oriented specifically to the production mechanisms after pp collisions at LHC.

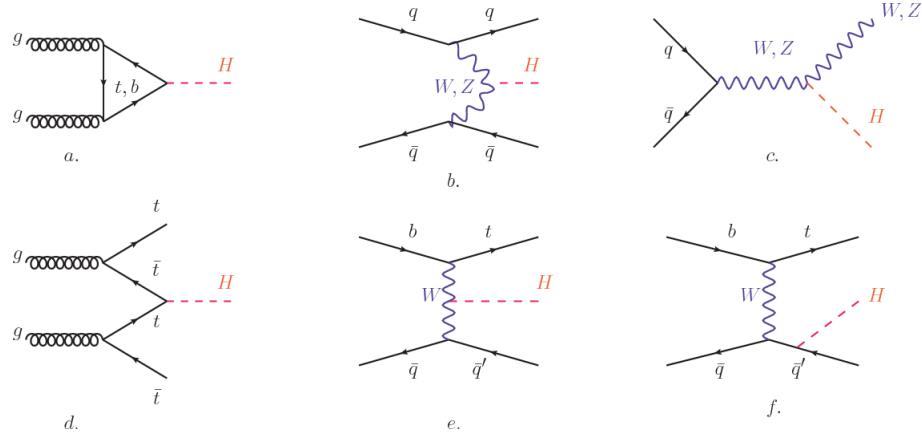


**Figure 2.11:** Main Higgs boson production mechanism Feynman diagrams. a. gluon-gluon fusion, b. vector boson fusion (VBF), c. Higgs-strahlung, d. Associated production with a top or bottom quark pair, e-f. associated production with a single top quark.

Figure 2.11 shows the Feynman diagrams for the leading order (first order) Higgs production processes at LHC, while the cross section for Higgs production as a function of the center of mass-energy ( $\sqrt{s}$ ) for pp collisions is showed in figure 2.12 left. The tags NLO (next to leading order), NNLO (next to next to leading order) and N3LO (next to next to next to leading order) make reference to the order at which

the perturbation series have been considered.

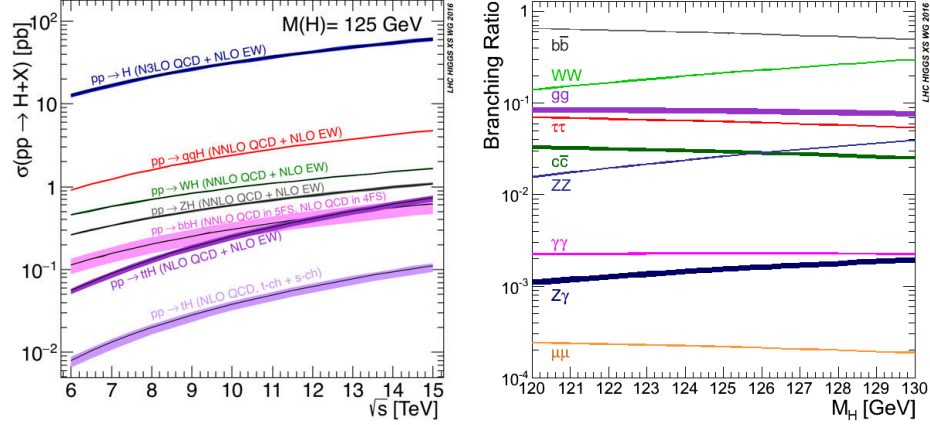


**Figure 2.12:** Higgs boson production cross sections (left) and decay branching ratios (right) for the main mechanisms. The VBF is indicated as  $q\bar{q}H$  [36].

As shown in eqns 2.47, 2.51 and 2.55, the strength of the Higgs-fermion interaction is proportional to the fermion mass while the strength of the Higgs-gauge boson interaction is proportional to the square of the gauge boson mass, which implies that the Higgs production and decay mechanisms are dominated by couplings  $H - (W, Z, t, b, \tau)$ .

The main production mechanism is the gluon fusion (figure 2.11a and  $pp \rightarrow H$  in figure 2.12) given that gluons carry the highest fraction of momentum of the protons in pp colliders. Since the Higgs boson does not couple to gluons, the mechanism proceeds through the exchange of a virtual top-quark loop given that for it the coupling is the biggest. Note that in this process, the Higgs boson is produced alone, which makes this mechanism experimentally clean when combined with the two-photon or the four-lepton decay channels (see section 2.3.7).

Vector boson fusion (figure 2.11b and  $pp \rightarrow q\bar{q}H$  in figure 2.12) has the second largest production cross section. The scattering of two fermions is mediated by a weak gauge boson which later emits a Higgs boson. In the final state, the two fermions

693 tend to be located in a particular region of the detector which is used as a signature  
 694 when analyzing the datasets provided by the experiments. More details about how  
 695 to identify events of interest in an analysis will be given in chapter ??.

696 The next production mechanism is Higgs-strahlung (figure 2.11c and  $pp \rightarrow WH, pp \rightarrow$   
 697  $ZH$  in figure 2.12) where two fermions annihilate to form a weak gauge boson. If the  
 698 initial fermions have enough energy, the emergent boson eventually will emit a Higgs  
 699 boson.

700 The associated production with a top or bottom quark pair and the associated pro-  
 701 duction with a single top quark (figure 2.11d-f and  $pp \rightarrow bbH, pp \rightarrow t\bar{t}H, pp \rightarrow tH$   
 702 in figure 2.12) have a smaller cross section than the main three mechanisms above,  
 703 but they provide a good opportunity to test the Higgs-top coupling. The analysis  
 704 reported in this thesis is developed using these production mechanisms. A detailed  
 705 description of the  $tH$  mechanism will be given in section 2.4.

### 706 2.3.7 Higgs boson decay channels

707 When a particle can decay through several modes, also known as channels, the  
 708 probability of decaying through a given channel is quantified by the “branching ratio  
 709 (BR)” of the decay channel; thus, the BR is defined as the ratio of number of decays  
 710 going through that given channel to the total number of decays. In regard to the  
 711 Higgs boson decay, the BR can be predicted with accuracy once the Higgs mass is  
 712 known [37, 38]. In figure 2.12 right, a plot of the BR as a function of the Higgs mass  
 713 is presented. The largest predicted BR corresponds to the  $b\bar{b}$  pair decay channel (see  
 714 table 2.9).



Decay channel	Branching ratio	Rel. uncertainty
$H \rightarrow b\bar{b}$	$5.84 \times 10^{-1}$	$+3.2\% - 3.3\%$
$H \rightarrow W^+W^-$	$2.14 \times 10^{-1}$	$+4.3\% - 4.2\%$
$H \rightarrow \tau^+\tau^-$	$6.27 \times 10^{-2}$	$+5.7\% - 5.7\%$
$H \rightarrow ZZ$	$2.62 \times 10^{-2}$	$+4.3\% - 4.1\%$
$H \rightarrow \gamma\gamma$	$2.27 \times 10^{-3}$	$+5.0\% - 4.9\%$
$H \rightarrow Z\gamma$	$1.53 \times 10^{-3}$	$+9.0\% - 8.9\%$
$H \rightarrow \mu^+\mu^-$	$2.18 \times 10^{-4}$	$+6.0\% - 5.9\%$

**Table 2.9:** Predicted branching ratios and the relative uncertainty for a SM Higgs boson with  $m_H = 125 \text{ GeV}/c^2$ . [9]

## 2.4 Associated production of a Higgs boson and a single Top quark.

Associated production of Higgs boson has been extensively studied [39–43]. While measurements of the main Higgs production mechanisms rates are sensitive to the strength of the Higgs coupling to W boson or top quark, they are not sensitive to the relative sign between the two couplings. In this thesis, the Higgs boson production mechanism explored is the associated production with a single top quark ( $th$ ) which offers sensitiveness to the relative sign of the Higgs couplings to W boson and to top quark. The description given here is based on the reference [41]

A process where two incoming particles interact and produce a final state with two particles can proceed in three ways also called channels (see, for instance, figure 2.13 omitting the red line). The t-channel represents processes where an intermediate particle is emitted by one of the incoming particles and absorbed by the other. The s-channel represents processes where the two incoming particles merge into an intermediate particle which eventually will split into the particles in the final state. The third channel, u-channel, is similar to the t-channel but the two outgoing particles

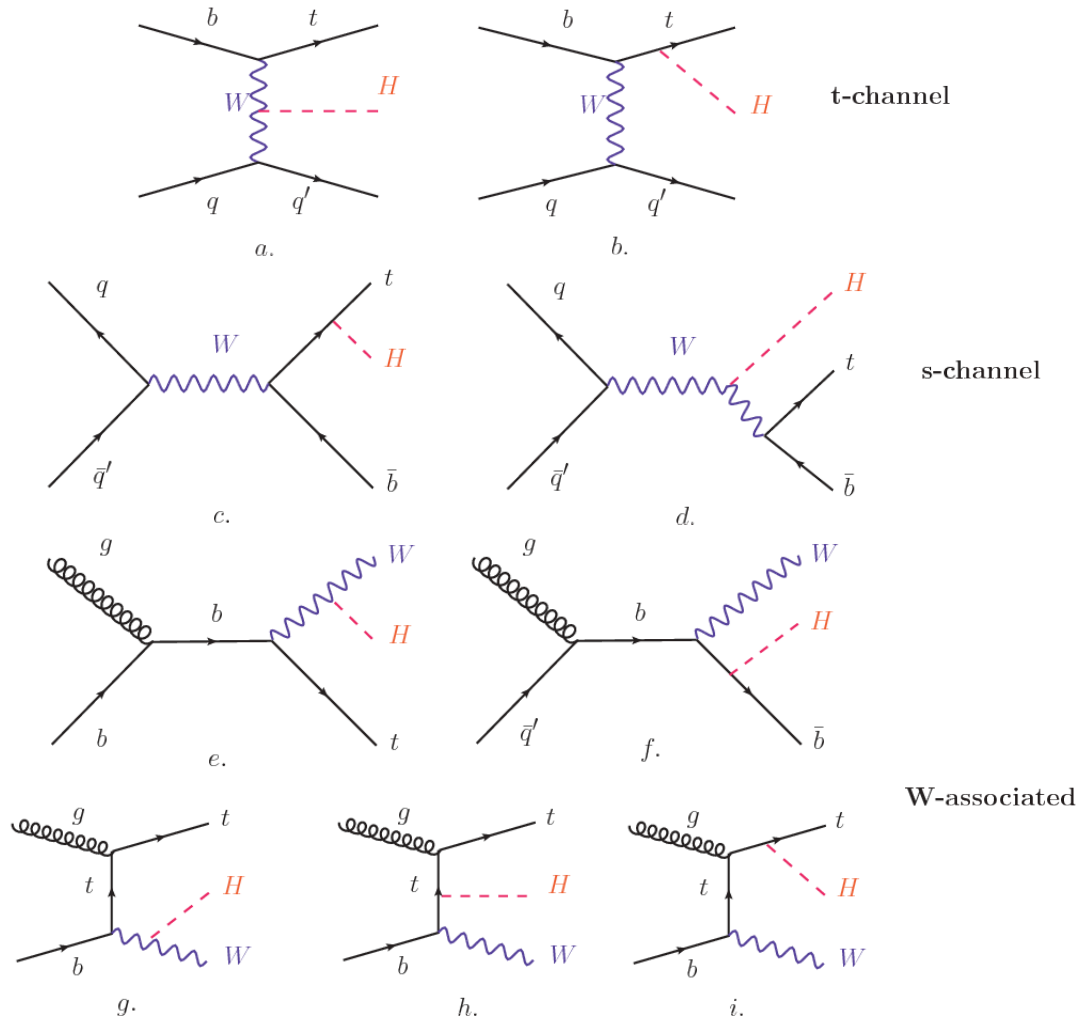


**Figure 2.13:** Associated Higgs boson production mechanism Feynman diagrams. a.,b. t-channel (tHq), c.,d. s-channel (tHb), e-i. W-associated.

733 interchange their roles.

734

735 The  $th$  production, where Higgs boson can be radiated either from the top quark or  
 736 from the  $W$  boson, is represented by the leading order Feynman diagrams in figure  
 737 2.13. The cross section for the  $th$  process is calculated, as usual, summing over  
 738 the contributions from the different feynman diagrams; therefore it depends on the  
 739 interference between the contributions. In the SM, the interference for t-channel (tHq

process) and W-associated (tHW process) production is destructive [39] resulting in the small cross sections presented in table 2.10.

tH production channel	Cross section (fb)
t-channel ( $pp \rightarrow tHq$ )	$70.79^{+2.99}_{-4.80}$
W-associated ( $pp \rightarrow tHW$ )	$15.61^{+0.83}_{-1.04}$
s-channel( $pp \rightarrow tHb$ )	$2.87^{+0.09}_{-0.08}$

**Table 2.10:** Predicted SM cross sections for  $tH$  production at  $\sqrt{s} = 13$  TeV [44, 45].

742

While the s-channel contribution can be neglected, it will be shown that a deviation from the SM destructive interference would result in an enhancement of the  $th$  cross section compared to that in SM, which could be used to get information about the sign of the Higgs-top coupling [41, 42]. In order to describe  $th$  production processes, Feynman diagram 2.13b will be considered; there, the W boson is radiated by a quark in the proton and eventually it will interact with the b quark. In the high energy regime, the effective W approximation [46] allows to describe the process as the emission of an approximately on-shell W and its hard scattering with the b quark; i.e.  $Wb \rightarrow th$ . The scattering amplitude for the process is given by

$$\mathcal{A} = \frac{g}{\sqrt{2}} \left[ (\kappa_t - \kappa_V) \frac{m_t \sqrt{s}}{m_W v} A\left(\frac{t}{s}, \varphi; \xi_t, \xi_b\right) + \left( \kappa_V \frac{2m_W}{v} \frac{s}{t} + (2\kappa_t - \kappa_V) \frac{m_t^2}{m_W v} \right) B\left(\frac{t}{s}, \varphi; \xi_t, \xi_b\right) \right], \quad (2.57)$$

where  $\kappa_V \equiv g_{HVV}/g_{HVV}^{SM}$  and  $\kappa_t \equiv g_{Ht}/g_{Ht}^{SM} = y_t/y_t^{SM}$  are scaling factors that quantify possible deviations of the couplings, Higgs-Vector boson (H-W) and Higgs-top (H-t) respectively, from the SM couplings;  $s = (p_W + p_b)^2$ ,  $t = (p_W - p_H)^2$ ,  $\varphi$  is the Higgs azimuthal angle around the  $z$  axis taken parallel to the direction of motion of the incoming W; A and B are functions describing the weak interaction in terms of

the chiral states of the quarks  $b$  and  $t$ . Terms that vanish in the high energy limit have been neglected as well as the Higgs and  $b$  quark masses<sup>8</sup>.

759

The scattering amplitude grows with energy like  $\sqrt{s}$  for  $\kappa_V \neq \kappa_t$ , in contrast to the SM ( $\kappa_t = \kappa_V = 1$ ), where the first term in 2.57 cancels out and the amplitude is constant for large  $s$ ; therefore, a deviation from the SM predictions represents an enhancement in the  $tHq$  cross section. In particular, for a SM H-W coupling and a H-t coupling of inverted sign with respect to the SM ( $\kappa_V = -\kappa_t = 1$ ) the  $tHq$  cross section is enhanced by a factor greater 10 as seen in the figure 2.14 taken from reference [41]; reference [47] has reported similar enhancement results.

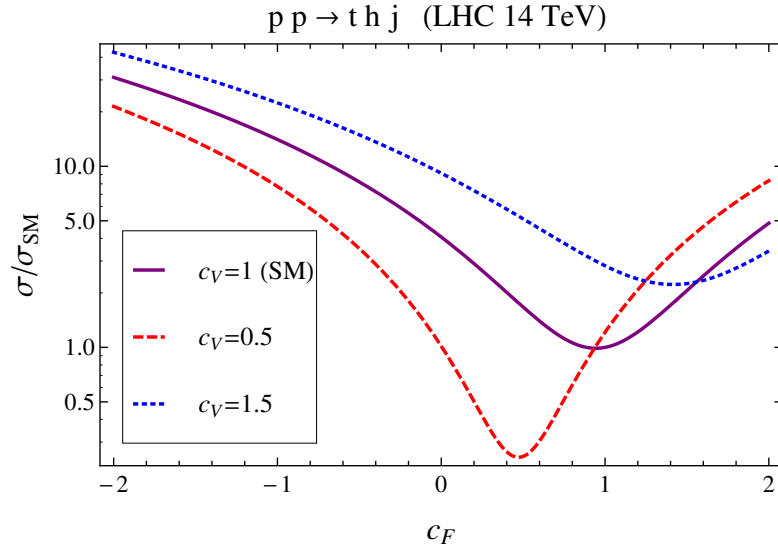


**Figure 2.14:** Cross section for  $tHq$  process as a function of  $\kappa_t$ , normalized to the SM, for three values of  $\kappa_V$ . In the plot  $c_f$  refers to the Higgs-fermion coupling which is dominated by the H-t coupling and represented here by  $\kappa_t$ . Solid, dashed and dotted lines correspond to  $c_V \rightarrow \kappa_V = 1, 0.5, 1.5$  respectively. Note that for the SM ( $\kappa_V = \kappa_t = 1$ ), the destructive effect of the interference is maximal.

A similar analysis is valid for the W-associated channel but, in that case, the interference is more complicated since there are more than two contributions and an ad-

<sup>8</sup> A detailed explanation of the structure and approximations used to derive  $\mathcal{A}$  can be found in reference [41]

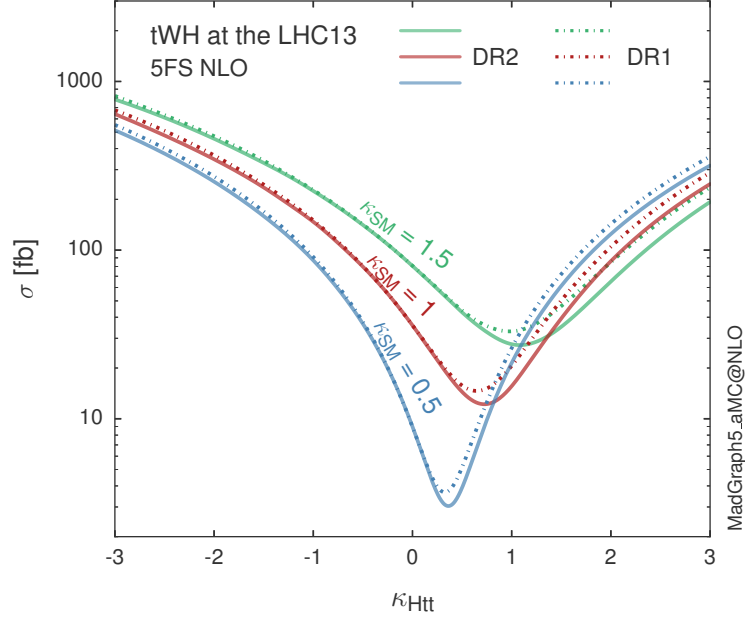


**Figure 2.15:** Cross section for  $tHW$  process as a function of  $\kappa_{Htt}$ , for three values of  $\kappa_{SM}$  at  $\sqrt{s} = 13$  TeV.  $\kappa_{Htt}^2 = \sigma_{Htt}/\sigma_{Htt}^{SM}$  is a simple rescaling of the SM Higgs interactions.

769 ditional interference with the production of Higgs boson and a top pair process( $t\bar{t}H$ ).  
 770 The calculations are made using the so-called Diagram Removal (DR) technique where  
 771 interfering diagrams are removed (or added) from the calculations in order to evaluate  
 772 the impact of the removed contributions. DR1 was defined to neglect  $t\bar{t}H$  interference  
 773 while DR2 was defined to take  $t\bar{t}H$  interference into account [48]. As shown in figure  
 774 2.15, the  $tHW$  cross section is enhanced from about 15 fb (SM:  $\kappa_{Htt} = 1$ ) to about  
 775 150 fb ( $\kappa_{Htt} = -1$ ). Differences between curves for DR1 and DR2 help to gauge the  
 776 impact of the interference with  $t\bar{t}H$ .

777 Results of the calculations of the  $tHq$  and  $tHW$  cross sections at  $\sqrt{s} = 13$  TeV can be  
 778 found in reference [49] and a summary of the results is presented in table 2.11.

779

	$\sqrt{s}$ TeV	$\kappa_t = 1$	$\kappa_t = -1$
$\sigma^{LO}(tHq)(\text{fb})$ [41]	8	$\approx 17.4$	$\approx 252.7$
	14	$\approx 80.4$	$\approx 1042$
$\sigma^{NLO}(tHq)(\text{fb})$ [41]	8	$18.28^{+0.42}_{-0.38}$	$233.8^{+4.6}_{-0.0}$
	14	$88.2^{+1.7}_{-0.0}$	$982.8^{+28}_{-0.0}$
$\sigma^{LO}(tHq)(\text{fb})$ [47]	14	$\approx 71.8$	$\approx 893$
$\sigma^{LO}(tHW)(\text{fb})$ [47]	14	$\approx 16.0$	$\approx 139$
$\sigma^{NLO}(tHq)(\text{fb})$ [49]	8	$18.69^{+8.62\%}_{-17.13\%}$	-
	13	$74.25^{+7.48\%}_{-15.35\%}$	$848^{+7.37\%}_{-13.70\%}$
	14	$90.10^{+7.34\%}_{-15.13\%}$	$1011^{+7.24\%}_{-13.39\%}$
$\sigma^{LO}(tHW)(\text{fb})$ [48]	13	$15.77^{+15.91\%}_{-15.76\%}$	-
$\sigma^{NLO}DR1(tHW)(\text{fb})$ [48]	13	$21.72^{+6.52\%}_{-5.24\%}$	$\approx 150$
$\sigma^{NLO}DR2(tHW)(\text{fb})$ [48]	13	$16.28^{+7.34\%}_{-15.13\%}$	$\approx 150$

**Table 2.11:** Predicted enhancement of the  $tHq$  and  $tHW$  cross sections at LHC for  $\kappa_V = 1$  and  $\kappa_t = \pm 1$  at LO and NLO; the cross section enhancement of more that a factor of 10 is due to the flipping in the sign of the H-t coupling with respect to the SM one.

## 2.5 The CP-mixing in $tH$ processes

In addition to the sensitivity to sign of the H-t coupling,  $tHq$  and  $tHW$  processes have been proposed as a tool to investigate the possibility of a H-t coupling that does not conserve CP [43, 48, 50]. Current experimental results are consistent with SM H-V and H-t couplings; however, negative H-t coupling is not excluded completely [52].

In this thesis, the sensitivity of  $th$  processes to CP-mixing is also studied in the effective field theory framework and based in references [43, 48]; a generic particle ( $X_0$ ) of spin-0 and a general CP violating interaction with the top quark, can couple to scalar and pseudoscalar fermionic densities. The H-W interaction is assumed to be SM-like. The Lagrangian modeling the H-t interaction is given by

$$\mathcal{L}_0^t = -\bar{\psi}_t (c_\alpha \kappa_{Htt} g_{Htt} + i s_\alpha \kappa_{Att} g_{Att} \gamma_5) \psi_t X_0, \quad (2.58)$$

791 where  $\alpha$  is the CP-mixing phase,  $c_\alpha \equiv \cos \alpha$  and  $s_\alpha \equiv \sin \alpha$ ,  $\kappa_{Htt}$  and  $\kappa_{Att}$  are real  
 792 dimensionless rescaling parameters<sup>9</sup>,  $g_{Htt} = g_{Att} = m_t/v = y_t/\sqrt{2}$  and  $v \sim 246$  GeV is  
 793 the Higgs vacuum expectation value. In this parametrization, it is easy to recover  
 794 three special cases

- 795 • CP-even coupling  $\rightarrow \alpha = 0^\circ$
- 796 • CP-odd coupling  $\rightarrow \alpha = 90^\circ$
- 797 • SM coupling  $\rightarrow \alpha = 0^\circ$  and  $\kappa_{Htt} = 1$

798 The loop induced  $X_0$  coupling to gluons can also be described in terms of the  
 799 parametrization above, according to

$$\mathcal{L}_0^g = -\frac{1}{4} \left( c_\alpha \kappa_{Hgg} g_{Hgg} G_{\mu\nu}^a G^{a,\mu\nu} + s_\alpha \kappa_{Agg} g_{Agg} G_{\mu\nu}^a \tilde{G}^{a,\mu\nu} \right) X_0. \quad (2.59)$$

800 where  $g_{Hgg} = -\alpha_s/3\pi v$  and  $g_{Agg} = \alpha_s/2\pi v$ . Under the assumption that the top quark  
 801 dominates the gluon-fusion process at LHC energies,  $\kappa_{Hgg} \rightarrow \kappa_{Htt}$  and  $\kappa_{Agg} \rightarrow \kappa_{Att}$ ,  
 802 so that the ratio between the gluon-gluon fusion cross section for  $X_0$  and for the SM  
 803 Higgs prediction can be written as

$$\frac{\sigma_{NLO}^{gg \rightarrow X_0}}{\sigma_{NLO,SM}^{gg \rightarrow H}} = c_\alpha^2 \kappa_{Htt}^2 + s_\alpha^2 \left( \kappa_{Att} \frac{g_{Agg}}{g_{Hgg}} \right)^2. \quad (2.60)$$

804 If the rescaling parameters are set to

$$\kappa_{Htt} = 1, \quad \kappa_{Att} = \left| \frac{g_{Hgg}}{g_{Agg}} \right| = \frac{2}{3}. \quad (2.61)$$

805 the gluon-fusion SM cross section is reproduced for every value of the CP-mixing  
 806 angle  $\alpha$ ; therefore, by imposing that condition to the Lagrangian density 2.58, the

---

<sup>9</sup> analog to  $\kappa_t$  and  $\kappa_V$

CP-mixing angle is not constrained by current data. Figure 2.16 shows the NLO cross sections for t-channel  $tX_0$  (blue) and  $t\bar{t}X_0$  (red) associated production processes as a function of the CP-mixing angle  $\alpha$ .  $X_0$  is a generic spin-0 particle with top quark CP-violating coupling. Rescaling factors  $\kappa_{Htt}$  and  $\kappa_{Att}$  have been set to reproduce the SM gluon-fusion cross sections.

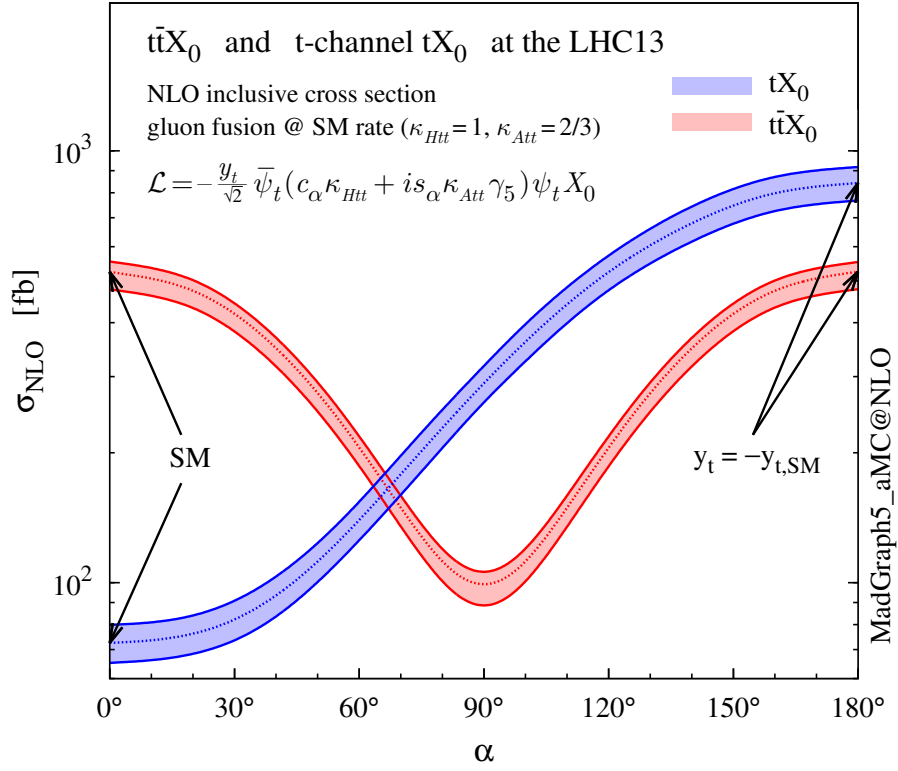


**Figure 2.16:** NLO cross sections for t-channel  $tX_0$  (blue) and  $t\bar{t}X_0$  (red) associated production processes as a function of the CP-mixing angle  $\alpha$ .  $X_0$  is a generic spin-0 particle with top quark CP-violating coupling [43].

It is interesting to notice that the  $tX_0$  cross section is enhanced, by a factor of about 10, when a continuous rotation in the scalar-pseudoscalar plane is applied; this enhancement is similar to the enhancement produced when the H-t coupling is flipped in sign with respect to the SM ( $y_t = -y_{t,SM}$  in the plot), as showed in section 2.4. In contrast, the degeneracy in the  $t\bar{t}X_0$  cross section is still present given that it depends



quadratically on the H-t coupling, but more interesting is to notice that  $t\bar{t}X_0$  cross section is exceeded by  $tX_0$  cross section after  $\alpha \sim 60^\circ$ .

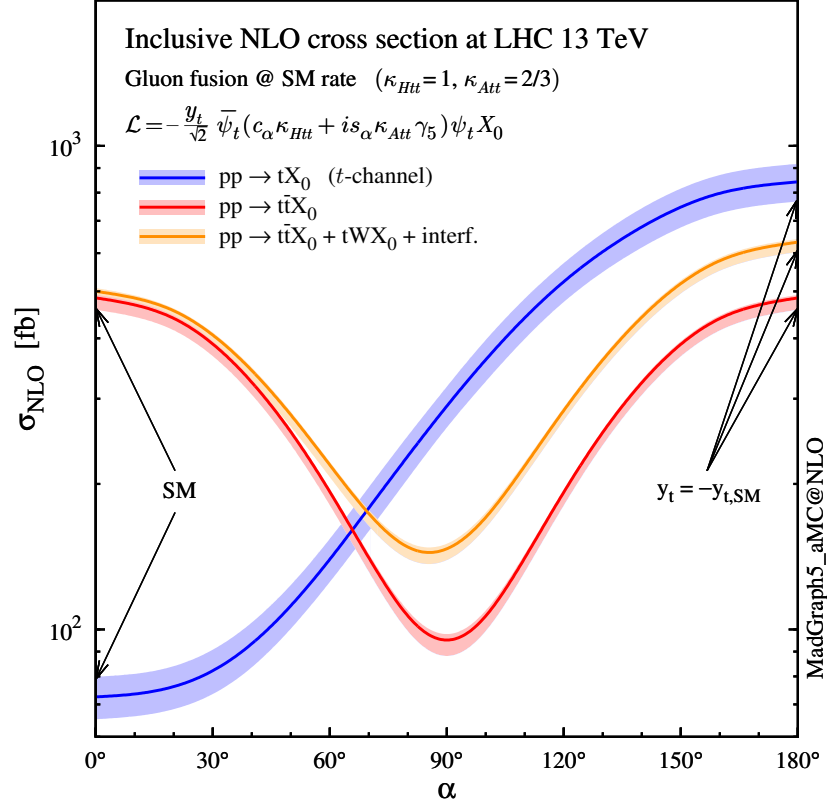


**Figure 2.17:** NLO cross sections for t-channel  $tX_0$  (blue),  $t\bar{t}X_0$  (red) associated production processes and combined  $tWX_0 + t\bar{t}X_0$  (including interference) production as a function of the CP-mixing angle  $\alpha$  [43].

818

819 A similar parametrization can be used to investigate the  $tHW$  process sensitivity to  
 820 CP-violating H-t coupling. As said in 2.4, the interference in the W-associated chan-  
 821 nel is more complicated because there are more than two contributions and also there  
 822 is interference with the  $t\bar{t}H$  production process.

823

824 Figure 2.17 shows the NLO cross sections for t-channel  $tX_0$  (blue),  $t\bar{t}X_0$  (red) asso-  
 825 ciated production and for the combined  $tWX_0 + t\bar{t}X_0 +$  interference (orange) as a  
 826 function of the CP-mixing angle. It is clear that the effect of the interference in the

combined case is the lifting of the degeneracy present in the  $t\bar{t}X_0$  production. The constructive interference enhances the cross section from about 500 fb at SM ( $\alpha = 0$ ) to about 600 fb ( $\alpha = 180^\circ \rightarrow y_t = -y_{t,SM}$ ). An analysis combining  $tHq$  and  $tHW$  processes will be made in this thesis taking advantage of the sensitivity improvement.

## 2.6 Experimental status of the anomalous Higg-fermion coupling.

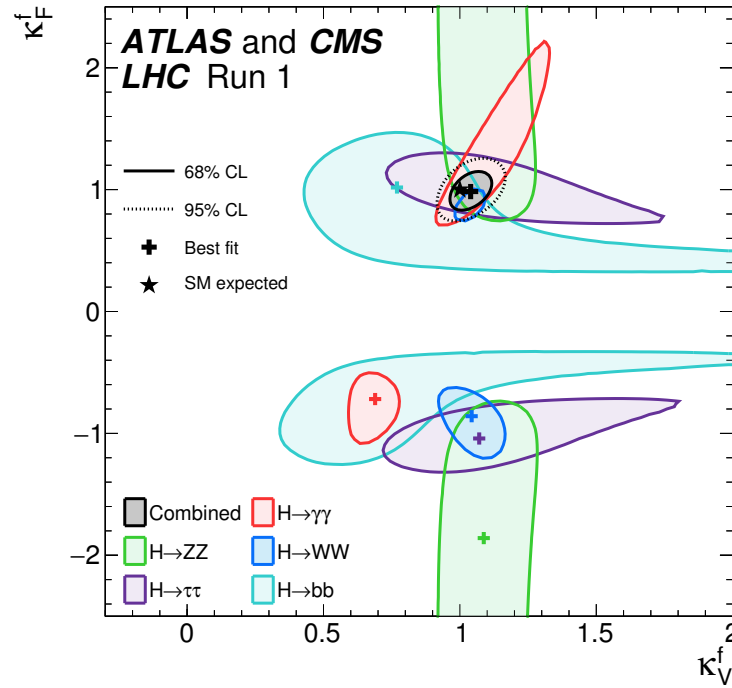


**Figure 2.18:** Combination of the ATLAS and CMS fits for coupling modifiers  $\kappa_t$ - $\kappa_V$ ; also shown the individual decay channels combination and their global combination. No assumptions have been made on the sign of the coupling modifiers [52].

ATLAS and CMS have performed analysis of the anomalous H-f coupling by making likelihood scans for the two coupling modifiers,  $\kappa_t$  and  $\kappa_V$ , under the assumption that

836  $\kappa_Z = \kappa_W = \kappa_V$  and  $\kappa_t = \kappa_\tau = \kappa_b = \kappa_f$ . Figure 2.18 shows the result of the combination  
 837 of ATLAS and CMS fits; also the individual decay channels combination and the  
 838 global combination results are shown.

839 While all the channels are compatible for positive values of the modifiers, for negative  
 840 values of  $\kappa_t$  there is no compatibility. The best fit for individual channels is compatible  
 841 with negative values of  $\kappa_t$  except for the  $H \rightarrow b\bar{b}$  channel which is expected to be the  
 842 most sensitive channel; therefore, the best fit for the global fit yields  $\kappa_t \geq 0$ . Thus,  
 843 the anomalous H-t coupling cannot be excluded completely.

## 844 References

- 845 [1] J. Schwinger. “Quantum Electrodynamics. I. A Covariant Formulation”. Phys-  
846 ical Review. 74 (10): 1439-61, (1948).
- 847 [2] R. P. Feynman. “Space-Time Approach to Quantum Electrodynamics”. Physical  
848 Review. 76 (6): 769-89, (1949).
- 849 [3] S. Tomonaga. “On a Relativistically Invariant Formulation of the Quantum  
850 Theory of Wave Fields”. Progress of Theoretical Physics. 1 (2): 27-42, (1946).
- 851 [4] D.J. Griffiths, “Introduction to electrodynamics”. 4th ed. Pearson, (2013).
- 852 [5] F. Mandl, G. Shaw. “Quantum field theory.” Chichester: Wiley (2009).
- 853 [6] F. Halzen, and A.D. Martin, “Quarks and leptons: An introductory course in  
854 modern particle physics”. New York: Wiley, (1984) .
- 855 [7] File: Standard\_Model\_of\_Elementary\_Particle\_dark.svg. (2017, June 12)  
856 Wikimedia Commons, the free media repository. Retrieved Novem-  
857 ber 27, 2017 from [https://www.collegiate-advanced-electricity.com/single-](https://www.collegiate-advanced-electricity.com/single-post/2017/04/10/The-Standard-Model-of-Particle-Physics)  
858 [post/2017/04/10/The-Standard-Model-of-Particle-Physics](https://www.collegiate-advanced-electricity.com/single-post/2017/04/10/The-Standard-Model-of-Particle-Physics).
- 859 [8] E. Noether, “Invariante Variationsprobleme”, Nachrichten von der Gesellschaft  
860 der Wissenschaften zu Göttingen, mathematisch-physikalische Klasse, vol. 1918,  
861 pp. 235-257, (1918).

- 862 [9] C. Patrignani et al. (Particle Data Group), *Chin. Phys. C*, 40, 100001 (2016)  
863 and 2017 update.
- 864 [10] M. Goldhaber, L. Grodzins, A.W. Sunyar “Helicity of Neutrinos”, *Phys. Rev.*  
865 109, 1015 (1958).
- 866 [11] Palanque-DeLabrouille N et al. “Neutrino masses and cosmology with Lyman-  
867 alpha forest power spectrum”, *JCAP* 11 011 (2015).
- 868 [12] M. Gell-Mann. “A Schematic Model of Baryons and Mesons”. *Physics Letters*.  
869 8 (3): 214-215 (1964).
- 870 [13] G. Zweig. “An SU(3) Model for Strong Interaction Symmetry and its Breaking”  
871 (PDF). CERN Report No.8182/TH.401 (1964).
- 872 [14] G. Zweig. “An SU(3) Model for Strong Interaction Symmetry and its Breaking:  
873 II” (PDF). CERN Report No.8419/TH.412(1964).
- 874 [15] M. Gell-Mann. “The Interpretation of the New Particles as Displaced Charged  
875 Multiplets”. *Il Nuovo Cimento* 4: 848. (1956).
- 876 [16] T. Nakano, K. Nishijima. “Charge Independence for V-particles”. *Progress of*  
877 *Theoretical Physics* 10 (5): 581-582. (1953).
- 878 [17] N. Cabibbo, “Unitary symmetry and leptonic decays” *Physical Review Letters*,  
879 vol. 10, no. 12, p. 531, (1963).
- 880 [18] M.Kobayashi, T.Maskawa, “CP-violation in the renormalizable theory of weak  
881 interaction,” *Progress of Theoretical Physics*, vol. 49, no. 2, pp. 652-657, (1973).
- 882 [19] File: Weak Decay (flipped).svg. (2017, June 12). Wikimedia Com-  
883 mons, the free media repository. Retrieved November 27, 2017 from

- 884 [https://commons.wikimedia.org/w/index.php?title=File:Weak\\_Decay\\_\(flipped\)](https://commons.wikimedia.org/w/index.php?title=File:Weak_Decay_(flipped).svg&oldid=247498592)  
885 [.svg&oldid=247498592](https://commons.wikimedia.org/w/index.php?title=File:Weak_Decay_(flipped).svg&oldid=247498592).
- 886 [20] Georgia Tech University. Coupling Constants for the Fundamental  
887 Forces(2005). Retrieved January 10, 2018, from [http://hyperphysics.phy-](http://hyperphysics.phy-astr.gsu.edu/hbase/Forces/couple.html#c2)  
888 [astr.gsu.edu/hbase/Forces/couple.html#c2](http://hyperphysics.phy-astr.gsu.edu/hbase/Forces/couple.html#c2)
- 889 [21] M. Strassler. (May 31, 2013). The Strengths of the Known Forces. Retrieved Jan-  
890 uary 10, 2018, from [https://profmattstrassler.com/articles-and-posts/particle-](https://profmattstrassler.com/articles-and-posts/particle-physics-basics/the-known-forces-of-nature/the-strength-of-the-known-forces/)  
891 [physics-basics/the-known-forces-of-nature/the-strength-of-the-known-forces/](https://profmattstrassler.com/articles-and-posts/particle-physics-basics/the-known-forces-of-nature/the-strength-of-the-known-forces/)
- 892 [22] S.L. Glashow. “Partial symmetries of weak interactions”, Nucl. Phys. 22 579-  
893 588, (1961).
- 894 [23] A. Salam, J.C. Ward. “Electromagnetic and weak interactions”, Physics Letters  
895 13 168-171, (1964).
- 896 [24] S. Weinberg, “A model of leptons”, Physical Review Letters, vol. 19, no. 21, p.  
897 1264, (1967).
- 898 [25] M. Peskin, D. Schroeder, “An introduction to quantum field theory”. Perseus  
899 Books Publishing L.L.C., (1995).
- 900 [26] A. Pich. “The Standard Model of Electroweak Interactions”  
901 <https://arxiv.org/abs/1201.0537>
- 902 [27] F.Bellaiche. (2012, 2 September). “What’s this Higgs boson anyway?”. Retrieved  
903 from: <https://www.quantum-bits.org/?p=233>
- 904 [28] M. Endres et al. Nature 487, 454-458 (2012) doi:10.1038/nature11255

- [29] F. Englert, R. Brout. “Broken Symmetry and the Mass of Gauge Vector Mesons”. Physical Review Letters. 13 (9): 321-23.(1964)  
doi:10.1103/PhysRevLett.13.321
- [30] P.Higgs. “Broken Symmetries and the Masses of Gauge Bosons”. Physical Review Letters. 13 (16): 508-509,(1964). doi:10.1103/PhysRevLett.13.508.
- [31] G.Guralnik, C.R. Hagen and T.W.B. Kibble. “Global Conservation Laws and Massless Particles”. Physical Review Letters. 13 (20): 585-587, (1964).  
doi:10.1103/PhysRevLett.13.585.
- [32] CMS collaboration. “Observation of a new boson at a mass of 125 GeV with the CMS experiment at the LHC”. Physics Letters B. 716 (1): 30-61 (2012).  
arXiv:1207.7235. doi:10.1016/j.physletb.2012.08.021
- [33] ATLAS collaboration. “Observation of a New Particle in the Search for the Standard Model Higgs Boson with the ATLAS Detector at the LHC”. Physics Letters B. 716 (1): 1-29 (2012). arXiv:1207.7214. doi:10.1016/j.physletb.2012.08.020.
- [34] ATLAS collaboration; CMS collaboration (26 March 2015). “Combined Measurement of the Higgs Boson Mass in pp Collisions at  $\sqrt{s}=7$  and 8 TeV with the ATLAS and CMS Experiments”. Physical Review Letters. 114 (19): 191803.  
arXiv:1503.07589. doi:10.1103/PhysRevLett.114.191803.
- [35] LHC International Masterclasses “When protons collide”. Retrieved from  
[http://atlas.physicsmasterclasses.org/en/zpath\\_protoncollisions.htm](http://atlas.physicsmasterclasses.org/en/zpath_protoncollisions.htm)
- [36] CMS Collaboration, “SM Higgs Branching Ratios and Total Decay Widths (up-date in CERN Report4 2016)”.

- 927 <https://twiki.cern.ch/twiki/bin/view/LHCPhysics/CERNYellowReportPageBR>  
928 , last accessed on 17.12.2017.
- 929 [37] R. Grant V. “Determination of Higgs branching ratios in  $H \rightarrow W^+W^- \rightarrow$   
930  $l\nu jj$  and  $H \rightarrow ZZ \rightarrow l^+l^-jj$  channels”. Physics Department, Uni-  
931 versity of Tennessee (Dated: October 31, 2012). Retrieved from  
932 <http://aesop.phys.utk.edu/ph611/2012/projects/Riley.pdf>
- 933 [38] LHC Higgs Cross Section Working Group, Denner, A., Heinemeyer, S. et al.  
934 “Standard model Higgs-boson branching ratios with uncertainties”. Eur. Phys.  
935 J. C (2011) 71: 1753. <https://doi.org/10.1140/epjc/s10052-011-1753-8>
- 936 [39] F. Maltoni, K. Paul, T. Stelzer, and S. Willenbrock, “Associated production  
937 of Higgs and single top at hadron colliders”, Phys.Rev. D64 (2001) 094023,  
938 [hep-ph/0106293].
- 939 [40] S. Biswas, E. Gabrielli, F. Margaroli, and B. Mele, “Direct constraints on the  
940 top-Higgs coupling from the 8 TeV LHC data,” Journal of High Energy Physics,  
941 vol. 07, p. 073, (2013).
- 942 [41] M. Farina, C. Grojean, F. Maltoni, E. Salvioni, and A. Thamm, “Lifting de-  
943 generacies in Higgs couplings using single top production in association with a  
944 Higgs boson,” Journal of High Energy Physics, vol. 05, p. 022, (2013).
- 945 [42] T.M. Tait and C.-P. Yuan, “Single top quark production as a window to physics  
946 beyond the standard model”, Phys. Rev. D 63 (2000) 014018 [hep-ph/0007298].
- 947 [43] F. Demartin, F. Maltoni, K. Mawatari, and M. Zaro, “Higgs production in  
948 association with a single top quark at the LHC,” European Physical Journal C,  
949 vol. 75, p. 267, (2015).



- 950 [44] CMS Collaboration, “Modelling of the single top-quark pro-  
 951 duction in association with the Higgs boson at 13 TeV.”  
 952 <https://twiki.cern.ch/twiki/bin/viewauth/CMS/SingleTopHiggsGeneration13TeV>,  
 953 last accessed on 16.01.2018.
- 954 [45] CMS Collaboration, “SM Higgs production cross sections at  $\sqrt{s} = 13$  TeV.”  
 955 <https://twiki.cern.ch/twiki/bin/view/LHCPhysics/CERNYellowReportPageAt13TeV>, last  
 956 accessed on 16.01.2018.
- 957 [46] S. Dawson, The effective W approximation, Nucl. Phys. B 249 (1985) 42.
- 958 [47] S. Biswas, E. Gabrielli and B. Mele, JHEP 1301 (2013) 088 [arXiv:1211.0499  
 959 [hep-ph]].
- 960 [48] F. Demartin, B. Maier, F. Maltoni, K. Mawatari, and M. Zaro, “tWH associated  
 961 production at the LHC”, European Physical Journal C, vol. 77, p. 34, (2017).  
 962 arXiv:1607.05862
- 963 [49] LHC Higgs Cross Section Working Group, “Handbook of LHC Higgs Cross  
 964 Sections: 4.Deciphering the Nature of the Higgs Sector”, arXiv:1610.07922.
- 965 [50] J. Ellis, D. S. Hwang, K. Sakurai, and M. Takeuchi. “Disentangling Higgs-Top  
 966 Couplings in Associated Production”, JHEP 1404 (2014) 004, [arXiv:1312.5736].
- 967 [51] CMS Collaboration, V. Khachatryan et al., “Precise determination of the mass  
 968 of the Higgs boson and tests of compatibility of its couplings with the standard  
 969 model predictions using proton collisions at 7 and 8 TeV,” arXiv:1412.8662.
- 970 [52] ATLAS and CMS Collaborations, “Measurements of the Higgs boson produc-  
 971 tion and decay rates and constraints on its couplings from a combined ATLAS

- 972 and CMS analysis of the LHC pp collision data at  $\sqrt{s} = 7$  and 8 TeV,” (2016).  
 973 CERN-EP-2016-100, ATLAS-HIGG-2015-07, CMS-HIG-15-002.
- 974 [53] File:Cern-accelerator-complex.svg. Wikimedia Commons,  
 975 the free media repository. Retrieved January, 2018 from  
 976 <https://commons.wikimedia.org/wiki/File:Cern-accelerator-complex.svg>
- 977 [54] J.L. Caron , “Layout of the LEP tunnel including future LHC infrastructures.”,  
 978 (Nov, 1993). A C Collection. Legacy of AC. Pictures from 1992 to 2002. Re-  
 979 trieved from <https://cds.cern.ch/record/841542>
- 980 [55] M. Vretenar, “The radio-frequency quadrupole”. CERN Yellow Report CERN-  
 981 2013-001, pp.207-223 DOI:10.5170/CERN-2013-001.207. arXiv:1303.6762
- 982 [56] L.Evans. P. Bryant (editors). “LHC Machine”. JINST 3 S08001 (2008).
- 983 [57] CERN Photographic Service.“Radio-frequency quadrupole, RFQ-1”, March  
 984 1983, CERN-AC-8303511. Retrieved from <https://cds.cern.ch/record/615852>.
- 985 [58] CERN Photographic Service “Animation of CERN’s accelerator net-  
 986 work”, 14 October 2013. DOI: 10.17181/cds.1610170 Retrieved from  
 987 <https://videos.cern.ch/record/1610170>
- 988 [59] C.Sutton. “Particle accelerator”.Encyclopedia Britannica. July 17, 2013. Re-  
 989 trieved from <https://www.britannica.com/technology/particle-accelerator>.
- 990 [60] L.Guiraud. “Installation of LHC cavity in vacuum tank.”. July 27 2000. CERN-  
 991 AC-0007016. Retrieved from <https://cds.cern.ch/record/41567>.
- 992 [61] J.L. Caron, “Magnetic field induced by the LHC dipole’s superconducting coils”.  
 993 March 1998. AC Collection. Legacy of AC. Pictures from 1992 to 2002. LHC-  
 994 PHO-1998-325. Retrieved from <https://cds.cern.ch/record/841511>

- 995 [62] AC Team. “Diagram of an LHC dipole magnet”. June 1999. CERN-DI-9906025  
996 retrieved from <https://cds.cern.ch/record/40524>.
- 997 [63] CMS Collaboration “Public CMS Luminosity Information”.  
998 <https://twiki.cern.ch/twiki/bin/view/CMSPublic/LumiPublicResults#2016>  
999 [\\_proton\\_proton\\_13\\_TeV\\_collis](#), last accessed 24.01.2018
- 1000 [64] J.L. Caron. “LHC Layout” AC Collection. Legacy of AC. Pictures  
1001 from 1992 to 2002. September 1997, LHC-PHO-1997-060. Retrieved from  
1002 <https://cds.cern.ch/record/841573>.
- 1003 [65] CMS Collaboration. “The CMS experiment at the CERN LHC” JINST 3 S08004  
1004 (2008).
- 1005 [66] CMS Collaboration. “CMS detector drawings 2012” CMS-PHO-GEN-2012-002.  
1006 Retrieved from <http://cds.cern.ch/record/1433717>.
- 1007 [67] R. Breedon. “View through the CMS detector during the cooldown of the  
1008 solenoid on February 2006. CMS Collection”, February 2006, CMS-PHO-  
1009 OREACH-2005-004, Retrieved from <https://cds.cern.ch/record/930094>.
- 1010 [68] A. Dominguez et. al. “CMS Technical Design Report for the Pixel Detector  
1011 Upgrade”, CERN-LHCC-2012-016. CMS-TDR-11.
- 1012 [69] CMS Collaboration. “Description and performance of track and primary-vertex  
1013 reconstruction with the CMS tracker,” Journal of Instrumentation, vol. 9, no.  
1014 10, p. P10009,(2014).
- 1015 [70] CMS Collaboration and M. Brice. “Images of the CMS Tracker Inner  
1016 Barrel”, November 2008, CMS-PHO-TRACKER-2008-002. Retrieved from  
1017 <https://cds.cern.ch/record/1431467>.

- 1018 [71] M. Weber. “The CMS tracker”. 6th international conference on hyperons, charm  
1019 and beauty hadrons Chicago, June 28-July 3 2004.
- 1020 [72] CMS Collaboration. “Projected Performance of an Upgraded CMS Detector at  
1021 the LHC and HL-LHC: Contribution to the Snowmass Process”. Jul 26, 2013.  
1022 arXiv:1307.7135
- 1023 [73] L. Veillet. “End assembly of HB with EB rails and rotation in-  
1024 side SX ”, January 2002. CMS-PHO-HCAL-2002-002. Retrieved from  
1025 <https://cds.cern.ch/record/42594>.
- 1026 [74] J. Puerta-Pelayo. “First DT+RPC chambers installation round in the  
1027 UX5 cavern.”. January 2007, CMS-PHO-OREACH-2007-001. Retrieved from  
1028 <https://cds.cern.ch/record/1019185>
- 1029 [75] X. Cid Vidal and R. Cid Manzano. “CMS Global Muon Trigger” web  
1030 site: Taking a closer look at LHC. Retrieved from [https://www.lhc-](https://www.lhc-closer.es/taking_a_closer_look_at_lhc/0.lhc_trigger)  
1031 [closer.es/taking\\_a\\_closer\\_look\\_at\\_lhc/0.lhc\\_trigger](https://www.lhc-closer.es/taking_a_closer_look_at_lhc/0.lhc_trigger)
- 1032 [76] WLCG Project Office, “Documents & Reference - Tiers - Structure,” (2014).  
1033 <http://wlcg.web.cern.ch/documents-reference> , last accessed on 30.01.2018.
- 1034 [77] CMS Collaboration, “Search for the associated production of a Higgs boson  
1035 with a single top quark in proton-proton collisions at  $\sqrt{s} = 8$  TeV”, JHEP 06  
1036 (2016) 177, doi:10.1007/JHEP06(2016)177, arXiv:1509.08159.
- 1037 [78] B. Stieger, C. Jorda Lope et al., “Search for Associated Production of a Single  
1038 Top Quark and a Higgs Boson in Leptonic Channels”, CMS Analysis Note CMS  
1039 AN-14-140, 2014.

- 1040 [79] M. Peruzzi, C. Mueller, B. Stieger et al., “Search for ttH in multilepton final  
1041 states at  $\sqrt{s} = 13$  TeV”, CMS Analysis Note CMS AN-16-211, 2016.
- 1042 [80] CMS Collaboration, “Search for H to bbar in association with a single top quark  
1043 as a test of Higgs boson couplings at  $\sqrt{s} = 13$  TeV”, CMS Physics Analysis  
1044 Summary CMS-PAS-HIG-16-019, 2016.
- 1045 [81] B. Maier, “SingleTopHiggProduction13TeV”, February, 2016.  
1046 <https://twiki.cern.ch/twiki/bin/viewauth/CMS/SingleTopHiggsGeneration13TeV>.
- 1047 [82] M. Peruzzi, F. Romeo, B. Stieger et al., “Search for ttH in multilepton final  
1048 states at  $\sqrt{s} = 13$  TeV”, CMS Analysis Note CMS AN-17-029, 2017.
- 1049 [83] B. WG, “BtagRecommendation80XReReco”, February, 2017.  
1050 <https://twiki.cern.ch/twiki/bin/view/CMS/BtagRecommendation80XReReco>.